to boiling state within 15 min. Polymerization was performed until approximately 40 mL of acetonitrile was distilled from the reaction system within 60 min. The product was then purified three times by the following processes: centrifugation, decantation, and resuspension in acetonitrile with ultrasonication. The purified product was dissolved in distilled water and filtered through a Millipore 0.8 μm filter. The filtrate was freeze-dried, and a white powder was obtained. C30 was synthesized by altering the amount of MBAAm to 20 wt % of the combined weight of monomer and cross-linker. In the case of PMAA, no cross-linker was added to the reaction mixture. The amounts of total monomer and cross-linker were maintained at 1 wt % relative to the reaction medium, and the amounts of AIBN were maintained at 2 wt % relative to the total monomer and cross-linker.

#### 4.2.2. H-Gd, C10-Gd, and C30-Gd

For the synthesis of **H-Gd**, 100 mg of PMAA was dissolved in 20 mL of anhydrous *N*,*N*-dimethylformamide (DMF) in a three-neck flask and stirred under argon. 267 mg (1.39 mmol) of 1-ethyl-3-(3-dimethylaminopropyl)carbodiimide hydrochloride (WSCD·HCl), 188 mg (1.39 mmol) of 1-hydroxybenzotriazole (HOBt), and 180 mg (1.39 mmol) of *N*,*N*-diisopropylethylamine (DIEA) were added to the solution. The molar quantity of these reagents was maintained at 1.2 equiv of carboxyl groups of the polymer. After 30 min, 3.0 mg (0.0050 mmol, 2.5 wt % of the weight of the polymer) of Gd(AEDO3A) and 2.0 mg (0.0070 mmol, 2.0 wt % of the weight of the polymer) of dansyl ethylenediamine were added to the mixture, which was stirred overnight at room temperature. The DMF was then evaporated under reduced pressure, and a yellow oil was obtained. The residue was dissolved in 1.0 M NaOH aq and then neutralized by 1.0 M HCl aq. The solution was purified by ultrafiltration using a Sartorius VIVASPIN (MWCO 3000). The supernatant was freeze-dried, and a white powder was obtained.

The synthetic procedures for **C10-Gd** and **C30-Gd** were identical to that of **H-Gd**, but required a different purification process. After the evaporation of DMF, **C10-Gd** and **C30-Gd** were purified by performing the following processes five times: centrifugation, decantation, and resuspension in methanol with ultrasonication. The products were then dissolved in 1.0 M NaOH aq and neutralized by 1.0 M HCl aq. Next, the solutions were centrifuged and washed with distilled water several times. The purified products were freeze-dried, and white powders were obtained.

Gd(AEDO3A) and dansyl ethylenediamine were synthesized according to previous reports.[18,19]

### 4.3. Fluorescence lifetime measurements

The fluorescence decay curve of **H-Gd** was acquired and fitted to the double-exponential Eq. 2. In the case of **C10-Gd** and **C30-Gd**, fluorescence decay curves were fitted with triple-exponential components because of the light scattering light.

$$I(t) = I_1 exp(-t/\tau_1) + I_2 exp(-t/\tau_2) \quad (2)$$

The weighted average fluorescence lifetime ($\tau_F$) was calculated using Eq. 3 by excluding the light scattering component. The lifetime of the scattering light was on the tens of picoseconds timescale, which is much shorter than the nanosecond timescale of the fluorescence lifetime.

$$\tau_F = \tau_1 I_1/(I_1 + I_2) + \tau_2 I_2/(I_1 + I_2) \quad (3)$$


## Acknowledgments

This work was partially supported by the Japan Society for the Promotion of Science (JSPS) through its 'Funding Program for World-Leading Innovative R&D on Science and Technology (FIRST) Program' and by the Ministry of Education, Culture, Sports, Science, and Technology (MEXT) of Japan (Grant No. 20675004, 21685019, and 22108519). The Takeda Science Foundation, the Mochida Memorial Foundation, and the Naito Foundation also provided support. The Asahi Glass Foundation provided financial support. Part of the present experiments was carried out in a facility at the Research Center for Ultra-High Voltage Electron Microscopy at Osaka University. S.O. received support from the Global COE Program 'Global Education and Research Center for Bio-Environmental Chemistry' of Osaka University and the JSPS Fellowship for Young Scientists.


## Supplementary data

Supplementary data associated with this article can be found, in the online version, at doi:10.1016/j.bmc.2011.12.005.

## References and notes


1. Lauffer, R. B. *Chem. Rev.* **1987**, *87*, 901.
2. Jun, Y.-w.; Lee, J.-H.; Cheon, J. *Angew. Chem., Int. Ed.* **2008**, *47*, 5122.
3. Louie, A. Y.; Hüber, M. M.; Ahrens, E. T.; Rothbächer, U.; Moats, R.; Jacobs, R. E.; Fraser, S. E.; Meade, T. J. *Nat. Biotechnol.* **2000**, *18*, 321.
4. Hanaoka, K.; Kikuchi, K.; Terai, T.; Komatsu, T.; Nagano, T. *Chem. Eur. J.* **2008**, *14*, 987.
5. Zhang, X.-A.; Lovejoy, K. S.; Jasanoff, A.; Lippard, S. J. *Proc. Natl. Acad. Sci. U.S.A.* **2007**, *104*, 10780.
6. Que, E. L.; Gianolio, E.; Baker, S. L.; Wong, A. P.; Aime, S.; Chang, C. J. *J. Am. Chem. Soc.* **2009**, *131*, 8527.
7. Zhang, S.; Wu, K.; Sherry, A. D. *Angew. Chem., Int. Ed.* **1999**, *38*, 3192.
8. Tóth, É.; Bolskar, R. D.; Borel, A.; González, G.; Helm, L.; Merbach, A. E.; Sitharaman, B.; Wilson, L. J. *J. Am. Chem. Soc.* **2005**, *127*, 799.
9. Aime, S.; Fedeli, F.; Sanino, A.; Terreno, E. *J. Am. Chem. Soc.* **2006**, *128*, 11326.
10. Okada, S.; Mizukami, S.; Kikuchi, K. *ChemBioChem* **2010**, *11*, 785.
11. Hu, Y.; Litwin, T.; Nagaraja, A. R.; Kwong, B.; Katz, J.; Watson, N.; Irvine, D. J. *Nano Lett.* **2007**, *7*, 3056.
12. Yang, X.; Chen, L.; Huang, B.; Bai, F.; Yang, X. *Polymer* **2009**, *50*, 3556.
13. Gota, C.; Okabe, K.; Funatsu, T.; Harada, Y.; Uchiyama, S. *J. Am. Chem. Soc.* **2009**, *131*, 2766.
14. Tanaka, K.; Kitamura, N.; Chujo, Y. *Macromolecules* **2010**, *43*, 6180.
15. Hoshino, Y.; Koide, H.; Urakami, T.; Kanazawa, H.; Kodama, T.; Oku, N.; Shea, K. J. *J. Am. Chem. Soc.* **2010**, *132*, 6644.
16. Oda, Y.; Kanaoka, S.; Sato, T.; Aoshima, S.; Kuroda, K. *Biomacromolecules* **2011**, *12*, 3581.
17. Liu, G.; Yang, X.; Wang, Y. *Polym. Int.* **2007**, *56*, 905.
18. Li, C.; Li, Y.-X.; Law, G.-L.; Man, K.; Wong, W.-T.; Lei, H. *Bioconjugate Chem.* **2006**, *17*, 571.
19. Shea, K. J.; Stoddard, G. J.; Shavelle, D. M.; Wakui, F.; Choate, R. M. *Macromolecules* **1990**, *23*, 4497.
20. Hu, Y.; Smith, G. L.; Richardson, M. F.; McCormick, C. L. *Macromolecules* **1997**, *30*, 3526.
21. Hu, Y.; Armentrout, R. S.; McCormick, C. L. *Macromolecules* **1997**, *30*, 3538.
22. Li, Y.-H.; Chan, L.-M.; Tyer, L.; Moody, R. T.; Himel, C. M.; Hercules, D. M. *J. Am. Chem. Soc.* **1975**, *97*, 3118.
23. Caravan, P. *Chem. Soc. Rev.* **2006**, *35*, 512.
24. Weber, G. *Biochem. J.* **1952**, *51*, 145.
25. Hu, Y.; Horie, K.; Ushiki, H. *Macromolecules* **1992**, *25*, 6040.
26. Oishi, M.; Hayashi, H.; Iijima, M.; Nagasaki, Y. *J. Mater. Chem.* **2007**, *17*, 3720.

DOI: 10.1002/asia.201100647

# Fluorogenic Protein Labeling through Photoinduced Electron Transfer-Based BL-Tag Technology

**Kalyan K. Sadhu,[a] Shin Mizukami,[a, b] Carolyn R. Lanam,[a] and Kazuya Kikuchi*[a, b]**

In recent years, protein labeling has been routinely performed with various fluorescent markers.[1] The labeling of proteins allows monitoring of the specific location, movement, and interaction of proteins with other intracellular components using fluorescence microscopy.[2] For several decades, the labeling strategy mostly dealt with green fluorescent protein (GFP) and its variants. In order to overcome the unaltered fluorescent property and uncontrolled expression time of GFP, small molecular probe-based labeling approaches for live-cell imaging methods have been developed.[3] However, most of the reported small-molecule labeling probes do not show different fluorescence properties for the labeled and unlabeled states. Fluorescein-based arsenical hairpin binder (FlAsH) and resorufin-based arsenical hairpin binder (ReAsH) are the pioneer techniques for fluorogenic protein labeling with small molecular probes.[4]

In our earlier studies, we developed a site-specific protein labeling technique that employs a genetically modified β-lactamase (BL-tag).[5] Mutation at a specific position in TEM-1 (class A β-lactamases) provides turn-on fluorogenic biosensors involving a β-lactam ring. The reaction of wild-type TEM-1 (WT TEM) with the β-lactam moiety involves acylation and deacylation steps.[6] We have utilized the BL-tag protein for covalent attachment with a substrate. Despite the similar molecular weights of the BL-tag and GFP, fluorogenicity can be introduced only through the BL-tag technology.

We have developed a fluorogenic mechanism based on aggregation–elimination processes for highly selective protein labeling with a fluorophore of desired color using the BL-tag technology. We have also shown a broad applicability of dinitrobenzene (DNB) as a quencher.[5c,d] However, the limitation of the technology is a slow fluorogenic response of the synthesized probes such as **CCDNB**, which carries a coumarin fluorophore moiety, a cephalosporin moiety, and DNB (Figure 1). The necessary incubation time for a cell imaging experiment using **CCDNB** was 60 minutes. To reduce the incubation time for the imaging experiments, we aimed at developing more sophisticated probes that possess the DNB quencher. Herein, we report two newly designed probes with shorter linkers compared to those of **CCDNB**. In addition, we modified slightly the quencher in one probe. The probe with the modified quencher showed a comparatively fast fluorogenicity in vitro and in live-cell imaging studies. Fluorescence lifetime measurements indicated a different quenching mechanism for the most active probe. A detailed analysis of this new fluorogenic mechanism revealed a photoinduced electron transfer (PET) process[7] from the fluorophore donor to the quencher acceptor.

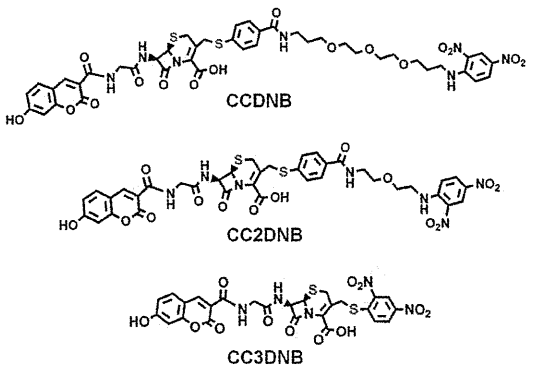


Figure 1. Chemical structures of the synthesized fluorescent probes used for protein labeling.

The two new probes **CC2DNB** and **CC3DNB** that have a comparatively short or no linker between the β-lactam and quencher, respectively, are depicted in Figure 1. 2-(2-Aminoethoxy)ethanamine was used as the linker between the cephalosporin part and the DNB quencher in **CC2DNB**. A coumarin derivative was attached to the opposite side of cephalosporin through a glycine linker to synthesize the **CC2DNB** probe. On the other hand, the synthesis of **CC3DNB** did not require any linker between the cephalosporin part and the quencher. 2,4-Dinitrothiophenol was directly introduced as a quencher to the cephalosporin part to synthesize **CC3DNB**.

[a] Dr. K. K. Sadhu, Dr. S. Mizukami, C. R. Lanam, Prof. Dr. K. Kikuchi
Division of Advanced Science and Biotechnology
Graduate School of Engineering
Osaka University
2-1 Yamadaoka, Suita, Osaka 565-0871 (Japan)
Fax: (+81) 6-6879-7875
E-mail: kkikuchi@mls.eng.osaka-u.ac.jp

[b] Dr. S. Mizukami, Prof. Dr. K. Kikuchi
Immunology Frontier Research Center
Osaka University
3-1 Yamadaoka, Suita, Osaka 565-0871 (Japan)

Supporting information for this article is available on the WWW under http://dx.doi.org/10.1002/asia.201100647.

Absorption spectra of **CC2DNB** and **CC3DNB** were recorded in 100 mM HEPES buffer (pH 7.4, Figure 2a) and methanol (Figure 2b), and compared with those of **CCDNB** under similar conditions. The reported absorption maxima of 348 nm for free *N*-ethyl-substituted 2,4-dinitroaniline[8]

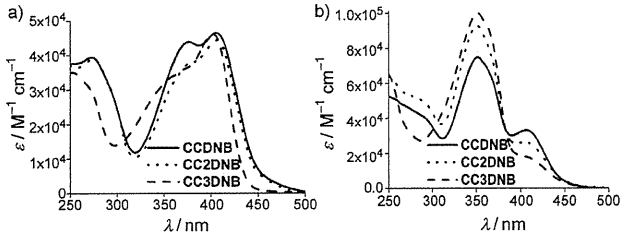


Figure 2. Absorbance spectra of **CCDNB**, **CC2DNB**, and **CC3DNB**. a) Spectra in 100 mM HEPES buffer (pH 7.4). b) Spectra in methanol.

and of 362 nm for 1-(methylthio)-2,4-dinitrobenzene[9] in methanol are quite similar to the observed absorption peaks at 350 nm in methanol for the synthesized probes containing the DNB part. In aqueous buffer, the absorption maxima for the coumarin and DNB parts of both **CCDNB** and **CC2DNB** were observed at 407 nm and 375 nm, respectively. Under the same conditions, the corresponding absorption peaks in **CC3DNB** were detected at 402 nm and 356 nm (shoulder band), respectively. The observed shift of the latter peak was due to the different DNB linkage in this probe. The slight blue shift in the absorption peak of coumarin in **CC3DNB** suggested a change in the interaction between the coumarin and DNB parts within this probe. Comparative measurements with the previously reported probe **CA**[5b] (Figures S3 and S4 in the Supporting Information) confirmed that the peaks around 356 nm or 375 nm in the new probes were due to the quencher DNB parts.

Next, we measured the fluorescence emission spectra of the free probes in 100 mM HEPES buffer of pH 7.4 (physiological pH) and compared them with those in methanol[10] (Figure S5 in the Supporting Information). The fluorescence signals of all the probes were sufficiently quenched in the aqueous buffer (Table 1). The strength of the interaction between the fluorophore and the quencher was comparable for **CCDNB** and **CC2DNB** due to the similar nature of the interacting parts. However, maximum fluorescence quenching was observed in the case of **CC3DNB**. The measured emission spectrum of **CA** in aqueous buffer (Figure S4 in the Supporting Information) confirmed the quenched state of the fluorophore in the newly synthesized probes.

Table 1. Fluorescence quantum yields of the synthesized probes in buffer of physiological pH and in methanol.

| Solvent | Fluorescence quantum yield ($\Phi$) | | |
|---|---|---|---|
| | **CCDNB**[5d] | **CC2DNB** | **CC3DNB** |
| 100 mM HEPES buffer (pH 7.4) | 0.04 | 0.04 | 0.02 |
| Methanol | 0.19 | 0.19 | 0.19 |

The fluorogenicities of the synthesized probes were studied by measuring the enhancement of the fluorescence intensity of each probe in the presence of the BL-tag and WT TEM. The reaction rates in the presence of WT TEM were faster for all three probes as compared to the rates in the presence of the BL-tag (Figure 3). In our earlier study, we found that the quencher part was eliminated from the **CCDNB** probe in the presence of the BL-tag.[5d] To modulate the elimination kinetics, the **CC2DNB** probe was synthesized with a much shorter linker compared to the previous polyethylene glycol spacer. However, there was only a slight enhancement in the reaction rate in the presence of the BL-tag. The rate of fluorescence enhancement with the BL-tag was the fastest for **CC3DNB** (Figure 3).

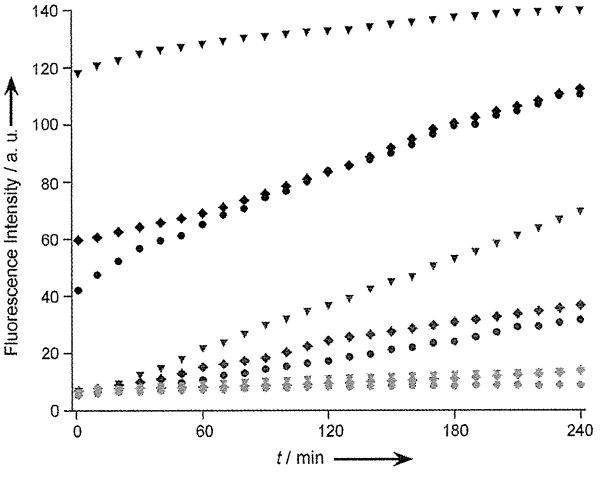


Figure 3. Change in the fluorescence intensities of **CCDNB**, **CC2DNB**, and **CC3DNB** (1 μM each) with time in the presence of WT TEM or BL-tag (0.5 μM each) in 100 mM HEPES buffer (pH 7.4) containing 0.1% DMSO at 25°C. Marker and color codes, circles: **CCDNB**, squares: **CC2DNB**, triangles: **CC3DNB**; black: WT TEM, dark grey: BL-tag, light grey: free probe.

The difference in the rates of fluorescence enhancement indicates that the removal of the quencher in **CC3DNB** is faster compared to the removal of the quencher in the other quenched probes. The overall stability of the eliminating groups partly controls the removal of quenchers from the probes. In the case of **CC3DNB**, the eliminating thiophenolate anion is sufficiently stabilized due to the presence of two highly electron-withdrawing nitro groups at the 2- and 4-positions. On the other hand, such stabilization was less pronounced in the **CCDNB** and **CC2DNB** probes owing to the less electron-withdrawing monosubstituted amide functional group at the 4-position of the thiophenol parts (Figure S6 in the Supporting Information).

The fluorescence enhancements of the different probes were not the same, even in the presence of WT TEM. Approximately 36% and 45% of the reactions were completed within 1 minute during the incubation of WT TEM with **CCDNB**[5d] and **CC2DNB**, respectively. The highest rate of

  

fluorescence enhancement was observed for the **CC3DNB** in the presence of WT TEM, with 88% of the catalytic reaction completed within 1 minute.

The labeling efficiency with each probe in the presence of the BL-tag was determined in vitro using SDS-PAGE. Incubation with the BL-tag protein for 30 minutes led to the elimination of the quencher in each probe and labeling of the tag protein with the same coumarin fluorophore through covalent linkage. Successful labeling of protein was verified for all three probes by visualization of protein bands in the gel upon irradiation with UV light ($\lambda_{ex}$=350 nm, see Figure 4). In each case, a fluorescent band at approximately

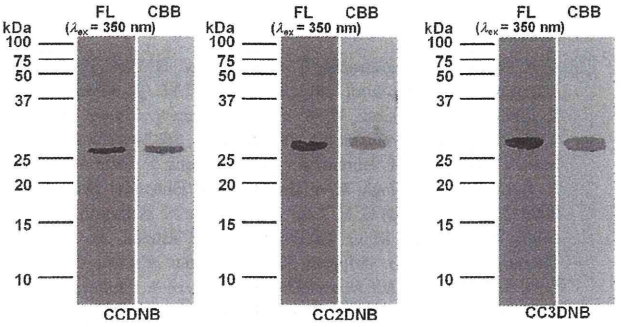


Figure 4. Gel images of BL-tag incubated with **CCDNB** (left), **CC2DNB** (middle), and **CC3DNB** (right) upon irradiation with UV light (FL) or after staining with Coomassie brilliant blue (CBB), as indicated on the top of each gel.

29 kDa was observed. Similar experiments carried out with WT TEM did not result in labeled protein. Because the relatively high rate of labeling with the **CC3DNB** probe compared to that with the other probes could not be completely understood from the in vitro analysis, further studies with living cells were performed.

For live-cell imaging experiments, we performed site-specific labeling of the transmembrane protein epidermal growth factor receptor (EGFR) fused with the BL-tag at the *N*-terminus, and observed labeling by confocal microscopy. To check the efficiencies of the synthesized probes, specific labeling of the cell membranes expressing the BL–EGFR fusion protein was assessed after 15 minutes of incubation with each probe (Figure 5). In the case of **CC3DNB**, sufficient protein labeling at the cell membrane was observed after this incubation period (Figure 5). However, for **CCDNB** and **CC2DNB**, cell membrane labeling was not sufficient after 15 minutes. Fluorescence images taken at 15-minute intervals confirmed sufficient labeling after 60 minutes of incubation with these probes (Figure S7 in the Supporting Information).

To check the origin of the different labeling efficiency among the probes, fluorescence decay profiles of the synthesized probes were obtained (Figure S9 in the Supporting Information). The data were compared with the fluorescence decay profile of **CA**. The **CA** probe, without any quencher, exhibited a single-exponential fluorescence decay. By contrast, the other fluorogenic probes exhibited biexponential decays due to the phenomenon of fluorescence quenching (Table S1 in the Supporting Information). The calculated average fluorescence lifetimes ($\tau$) of the **CCDNB** and **CC2DNB** probes were very close to that of **CA** (Table 2).

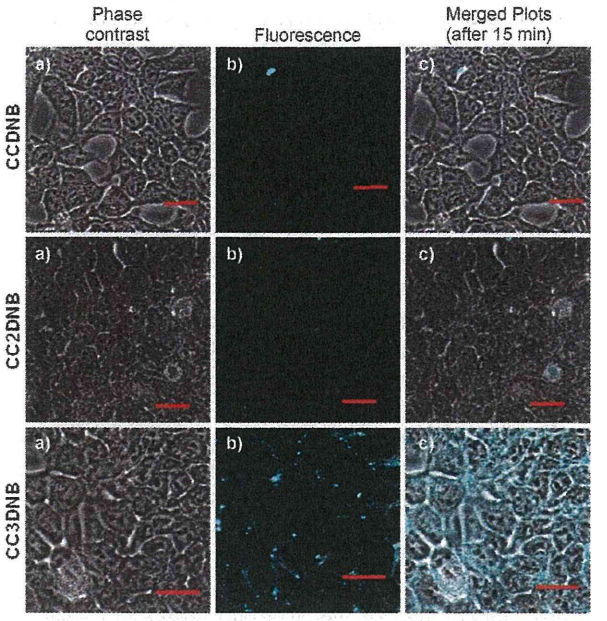


Figure 5. Confocal microscopic images of **CCDNB**-labeled (top), **CC2DNB**-labeled (middle), and **CC3DNB**-labeled (bottom) HEK293T cells expressing BL-tag–EGFR fusion protein after 15 min of incubation. a) Phase-contrast microscopic images, b) fluorescence microscopic images, and c) merged images. For fluorescence microscopic images, the cells were excited at 405 nm. Scale bars: 20 μm.

Table 2. Radiative and nonradiative rate constants of the synthesized probes in 100 mM HEPES buffer (pH 7.4) at 25°C.

| Probe | $\Phi$ | Avg $\tau$ [ns] | $k_r$ [$s^{-1}$] | $k_{nr}$ [$s^{-1}$] |
|---|---|---|---|---|
| **CA** | 0.4[5b] | 3.25 | $1.2\times10^8$ | $1.9\times10^8$ |
| **CCDNB** | 0.04[5d] | 3.60 | $1.1\times10^7$ | $2.6\times10^8$ |
| **CC2DNB** | 0.04 | 3.00 | $1.3\times10^7$ | $3.2\times10^8$ |
| **CC3DNB** | 0.02 | 0.39 | $5.1\times10^7$ | $2.5\times10^9$ |

The radiative decay rate constants ($k_r$) were significantly lower in **CCDNB** and **CC2DNB** compared to that of the **CA**. This can be attributed to an aggregation between the coumarin fluorophore and the DNB quencher of these two probes, a phenomenon quite similar to static aggregation-based quenching,[11] which is probably due to the π–π stacking interaction between the fluorophore and quencher.

In the case of the **CC3DNB** probe, both the average fluorescence lifetime and quantum yield decreased significantly compared to those of **CA**. This is due to the dynamic quenching process[11] operating in the **CC3DNB** probe. The radiative ($k_r$) and nonradiative ($k_{nr}$) decay rate constant values (Table 2) confirmed the existence of a different quenching mechanism in **CC3DNB** compared to that in

  

**CCDNB** and **CC2DNB**. The radiative decay rate constant of **CC3DNB** was slightly increased in comparison to those of the other quenched probes. This result confirmed that the aggregation between the quencher and the fluorophore in **CC3DNB** was not affected too much. However, the nonradiative decay rate constant in **CC3DNB** was much higher compared to those in all other probes. This dynamic quenching can be explained by an effective photoinduced electron transfer (PET) process from the coumarin donor to the DNB acceptor. This phenomenon is well known to occur with coumarin probes.[12]

According to the Rehm–Weller equation,[7] the rate of the PET reaction from coumarin to DNB is governed by the energy of the excited state species ($\Delta G_{00}$), the ground state oxidation potential of the coumarin donor ($E_{D^+/D}$), the reduction potential of the DNB acceptor ($E_{A/A^-}$), and the coulombic attraction energy ($E_{coul}$). On the basis of the experimental data for the excited state energy ($\Delta G_{00}=2.93$ eV) and the available data for the oxidation potential of 7-hydroxycoumarin[12b] ($E_{D^+/D}=0.67$ V vs. SCE) and for the reduction potential of DNB,[13] ($E_{A/A^-}=-0.88$ V vs. SCE), the Gibbs energy ($\Delta G$) for the electron transfer in a polar environment[7] ($E_{coul}=0.03$ eV) was found to be approximately −1.35 eV. This value was sufficiently negative for operating the diffusion-controlled electron-transfer process at ambient temperature. The shortening of the linker chain length in **CC3DNB** led to an effective PET process. The quencher did not directly interact with the fluorophore in the PET process like it did in the previous aggregation mode. This phenomenon was reflected in the faster recognition of the tag protein in the new PET-based probe. The probability of fluorescence resonance energy transfer (FRET) from coumarin to the DNB group can be ruled out due to the small overlap integral ($J=2\times10^{-23}\,M^{-1}\,cm^3$, Figure S10 in the Supporting Information) between the coumarin donor emission in **CC3DNB** and the acceptor DNB absorbance of compound **12** (probe without coumarin, Scheme S2 in the Supporting Information).

In summary, we have developed new fluorogenic probes valuable for protein labeling through our developed BL-tag technology. We reduced the linker chain length and slightly modified the quencher with regard to the probe previously reported by us, **CCDNB**. The probe with the shortest linker, **CC3DNB,** was found to be most effective, resulting in fast kinetics. The quenching mechanism in this probe was demonstrated as a PET process, which is different from the FRET- or static aggregation-based quenching occurring in the other probes. Thus, the new probe overcomes the limitation of the previous coumarin probes that required a long incubation period. In principle, such PET-based probe design could lead to the development of multi-colored fluorogenic probes for successful use in next-generation live-cell imaging technologies.

## Acknowledgements

This research was supported by the Japan Society for the Promotion of Science (JSPS) through its "Funding Program for World-Leading Innovative R&D on Science and Technology (FIRST Program)." This work was supported in part by the CREST funding program from the Japan Science and Technology Agency (JST); a Grant-in-Aid for Scientific Research from the Ministry of Education, Culture, Sports, Science and Technology (MEXT) of Japan; and a Grant-in-Aid from the Ministry of Health, Labour and Welfare (MHLW) of Japan. K.K.S. acknowledges support from a Global COE Fellowship of Osaka University. C.R.L. acknowledges a JASSO Fellowship.

**Keywords:** biotechnology · electron transfer · fluorescence spectroscopy · fluorescent probesprotein labeling

[1] a) A. Keppler, S. Gendreizig, T. Gronemeyer, H. Pick, H. Vogel, K. Johnsson, *Nat. Biotechnol.* **2003**, *21*, 86–89; b) L. W. Miller, J. Sable, P. Goelet, M. P. Sheetz, V. W. Cornish, *Angew. Chem.* **2004**, *116*, 1704–1707; *Angew. Chem. Int. Ed.* **2004**, *43*, 1672–1675; c) C. Hoffman, G. Gaietta, M. Bunemann, S. R. Adams, S. Oberdolff-Maass, B. Behr, J.-P. Vilardaga, R. Y. Tsien, M. H. Ellisman, *Nat. Methods* **2005**, *2*, 171–176; d) G. V. Los, A. Darzins, N. Karassina, C. Zimprich, R. Learish, M. G. McDougall, L. P. Encell, R. Friedman-Ohana, M. Wood, G. Vidugiris, K. Zimmerman, P. Otto, D. H. Klaubert, K. V. Wood, *Cell Notes* **2005**, *11*, 2–6; e) A. Ojida, K. Honda, D. Shinmi, S. Kiyonaka, Y. Mori, I. Hamachi, *J. Am. Chem. Soc.* **2006**, *128*, 10452–10459; f) S. R. Adams, R. Y. Tsien, *Nat. Protoc.* **2008**, *3*, 1527–1534; g) X. Zhou, X. Jin, D. Li, X. Wu, *Chem. Commun.* **2011**, *47*, 3921–3923.

[2] a) D. Summerer, S. Chen, N. Wu, A. Deiters, J. W. Chin, P. G. Schultz, *Proc. Natl. Acad. Sci. USA* **2006**, *103*, 9785–9789; b) C. Smith, *Nat. Methods* **2007**, *4*, 755–761; c) Z. Zhou, A. Koglin, Y. Wang, A. P. McMahon, C. T. Walsh, *J. Am. Chem. Soc.* **2008**, *130*, 9925–9930; d) R. McRae, P. Bagchi, S. Sumalekshmy, C. J. Fahrni, *Chem. Rev.* **2009**, *109*, 4780–4827; e) H. Ren, F. Xiao, K. Zhan, Y.-P. Kim, H. Xie, Z. Xia, J. Rao, *Angew. Chem.* **2009**, *121*, 9838–9842; *Angew. Chem. Int. Ed.* **2009**, *48*, 9658–9662; f) R. W. Watkins, L. D. Lavis, V. M. Kung, G. V. Los, R. T. Raines, *Org. Biomol. Chem.* **2009**, *7*, 3969–3975; g) D. Maurel, S. Banala, T. Laroche, K. Johnsson, *ACS Chem. Biol.* **2010**, *5*, 507–516; h) C. Uttamapinant, K. A. White, H. Baruah, S. Thompson, M. Fernández-Suárez, S. Puthenveetil, A. Y. Ting, *Proc. Natl. Acad. Sci. USA* **2010**, *107*, 10914–10919; i) D. Srikun, A. E. Albers, C. I. Nam, A. T. Iavarone, C. J. Chang, *J. Am. Chem. Soc.* **2010**, *132*, 4455–4465.

[3] a) C. Szent-Gyorgyi, B. F. Schmidt, Y. Creeger, G. W. Fisher, K. L. Zakel, S. Adler, J. A. Fitzpatrick, C. A. Woolford, Q. Yan, K. V. Vasilev, P. B. Berget, M. P. Bruchez, J. W. Jarvik, A. Waggoner, *Nat. Biotechnol.* **2008**, *26*, 235–240; b) O. Tour, S. R. Adams, R. A. Kerr, R. M. Meijer, T. J. Sejnowski, R. W. Tsien, R. Y. Tsien, *Nat. Chem. Biol.* **2007**, *3*, 423–431; c) N. T. Calloway, M. Choob, A. Sanz, M. P. Sheetz, L. W. Miller, V. W. Cornish, *ChemBioChem* **2007**, *8*, 767–774; d) N. Johnsson, K. Johnsson, *ACS Chem. Biol.* **2007**, *2*, 31–38; e) G. V. Los, L. P. Encell, M. G. McDougall, D. D. Hartzell, N. Karassina, C. Zimprich, M. G. Wood, R, Learish, R. F. Ohana, M. Urh, D. Simpson, J. Mendez, K. Zimmerman, P. Otto, G. Vidugiris, J. Zhu, A. Darzins, D. H. Klaubert, R. F. Bulleit and K. V. Wood, *ACS Chem. Biol.* **2008**, *3*, 373–382; f) M. A. Brun, K.-T. Tan, E. Nakata, M. J. Hinner, K. Johnsson, *J. Am. Chem. Soc.* **2009**, *131*, 5873–5884; g) S. S. Gallagher, J. E. Sable, M. P. Sheetz, V. W. Cornish, *ACS Chem. Biol.* **2009**, *4*, 547–556; h) H. E. Rajapakse, D. R. Reddy, S. Mohandessi, N. G. Butlin, L. W. Miller, *Angew. Chem.* **2009**, *121*, 5090–5092; *Angew. Chem. Int. Ed.* **2009**, *48*, 4990–4992; i) M. Bannwarth, I. R. Corrêa Jr., M. Sztretye, S. Pouvreau, C. Fellay, A. Aebischer, L. Royer, E. Ríos, K. Johnsson, *ACS Chem. Biol.* **2009**, *4*, 179–190; j) K. K. Sadhu, S. Mizukami, Y. Hori, K. Kikuchi, *Chem-*

  

*BioChem* **2011**, *12*, 1031–1034; k) C. Grunwald, K. Schulze, G. Giannone, L. Cognet, B. Lounis, D. Choquet, R. Tampé, *J. Am. Chem. Soc.* **2011**, *133*, 8090–8093; l) T. Komatsu, K. Johnsson, H. Okuno, H. Bito, T. Inoue, T. Nagano, Y. Urano, *J. Am. Chem. Soc.* **2011**, *133*, 6745–6751.

[4] a) B. A. Griffin, S. R. Adams, R. Y. Tsien, *Science* **1998**, *281*, 269–272; b) S. R. Adams, R. E. Campbell, L. A. Gross, B. R. Martin, G. K. Walkup, Y. Yao, J. Llopis, R. Y. Tsien, *J. Am. Chem. Soc.* **2002**, *124*, 6063–6076.

[5] a) S. Mizukami, S. Watanabe, Y. Hori, K. Kikuchi, *J. Am. Chem. Soc.* **2009**, *131*, 5016–5017; b) S. Watanabe, S. Mizukami, Y. Hori, K. Kikuchi, *Bioconjugate Chem.* **2010**, *21*, 2320–2326; c) K. K. Sadhu, S. Mizukami, S. Watanabe, K. Kikuchi, *Chem. Commun.* **2010**, *46*, 7403–7405; d) K. K. Sadhu, S. Mizukami, S. Watanabe, K. Kikuchi, *Mol. BioSyst.* **2011**, *7*, 1766–1772; e) A. Yoshimura, S. Mizukami, Y. Hori, S. Watanabe, K. Kikuchi, *ChemBioChem* **2011**, *12*, 1031–1034; f) S. Watanabe, S. Mizukami, Y. Akimoto, Y. Hori, K. Kikuchi, *Chem. Eur. J.* **2011**, *17*, 8342–8349; g) S. Mizukami, T. Yamamoto, A. Yoshimura, S. Watanabe, K. Kikuchi, *Angew. Chem.* **2011**, *123*, 8909–8911; *Angew. Chem. Int. Ed.* **2011**, *50*, 8750–8752.

[6] a) G. Guillaume, M. Vanhove, J. Lamotte-Brasseur, P. Ledent, M. Jamin, B. Joris, J.-M. Frère, *J. Biol. Chem.* **1997**, *272*, 5438–5444; b) H. Adachi, T. Ohta, H. Matsuzawa, *J. Biol. Chem.* **1991**, *266*, 3186–3191.

[7] D. Rehm, A. Weller, *Isr. J. Chem.* **1970**, *8*, 259–271.

[8] G. Punte, B. E. Rivero, *Acta Crystallogr. Sect. C* **1989**, *45*, 1952–1957.

[9] R. L. Gupta, B. H. K. Saini, T. R. Juneja, *Mutat. Res.* **1997**, *381*, 41–47.

[10] S. V. Balasubramanian, J. L. Alderfer, R. M. Straubinger, *J. Pharm. Sci.* **1994**, *83*, 1470–1476.

[11] S. Doose, H. Neuweiler, M. Sauer, *ChemPhysChem* **2009**, *10*, 1389–1398.

[12] a) J. R. Lakowicz, *Principles of Fluorescence Spectroscopy, 3rd ed.*, Springer Science+Business Media, LLC, **2006**; b) G. J. Smith, Y. Tang, J. M. Dyer, S. M. Scheele, *Photochem. Photobiol.* **2011**, *87*, 45–50.

[13] M. E. Peover, *Trans. Faraday Soc.* **1964**, *60*, 479–483.

Received: July 28, 2011
Published online: December 20, 2011

  

ChemComm

View Online / Journal Homepage / Table of Contents for this issue
Dynamic Article Links

Cite this: *Chem. Commun.*, 2012, **48**, 2234–2236

www.rsc.org/chemcomm

COMMUNICATION

# A long-lived luminescent probe to sensitively detect arylamine *N*-acetyltransferase (NAT) activity of cells†

**Takuya Terai,[a] Kazuya Kikuchi,[b] Yasuteru Urano,[c] Hirotatsu Kojima[d] and Tetsuo Nagano*[a]**

*Received 6th December 2011, Accepted 5th January 2012*
**DOI: 10.1039/c2cc17622j**



**Arylamine *N*-acetyltransferase (NAT) is an important phase II metabolizing enzyme that influences drug efficacy and adverse effects. Here, we report a long-lived luminescent lanthanide complex as a probe for NAT, employing an intraligand photo-induced electron transfer strategy. The probe shows approximately 100-fold increase of luminescence upon *N*-acetylation catalyzed by NAT, with relatively high specificity for NAT2 over NAT1. It is the first NAT probe that is suitable for sensitive, homogeneous, and rapid detection of NAT activity of recombinant enzyme or cell lysate, and is expected to be useful for drug discovery and clinical diagnosis.**

Arylamine *N*-acetyltransferases (NATs, EC 2.3.1.5) catalyse transfer of an acetyl group from acetyl CoA to aromatic amines, including pharmaceutical drugs and carcinogens.[1] In humans, two NATs (NAT1 and NAT2) are expressed, and both are principal phase II drug-metabolizing enzymes. NAT2 is a polymorphic enzyme that contributes to inter-individual differences in efficacy and adverse effects of various drugs. Polymorphism and differences in expression levels of NAT1 play a role in cancer progression.[2] Hence, a rapid and sensitive method to measure NAT activity is urgently required for efficient drug discovery, as well as for clinical diagnosis.

Currently, the most widely used method to quantify NAT activity is HPLC, using substrates such as 4-aminobenzoic acid (PABA, for NAT1),[3] 4-aminosalicylic acid (PAS, for NAT1),[4] and sulfamethazine (SMZ, for NAT2).[5] However, homogeneous assays using fluorogenic probes[6] are far more advantageous for high-throughput evaluation of enzyme activity with a microplate reader. To date, several fluorescent probes for NATs have been reported, including 2-aminoanthracene,[7] cresyl violet[8] and amonafide,[9] but all of them are susceptible to interference from biological components because their fluorescence lifetimes are less than a few nanoseconds. This drawback, we believe, prevents them from being sensitive enough for wide application.

Here, to address this problem, we report a novel probe for NAT based on a luminescent lanthanide complex. Lanthanide complexes, in particular those incorporating $Tb^{3+}$ or $Eu^{3+}$, emit characteristic luminescence in the visible to near-infrared region,[10,11] with a long lifetime (up to a few ms) and a large Stokes shift (> 300 nm). In general, lanthanide ions in luminescent complexes are excited indirectly *via* energy transfer from an organic chromophore, called an antenna, due to the low extinction coefficients of the forbidden f–f transitions.[10]

Recently, $Tb^{3+}$ and $Eu^{3+}$ complexes that exhibit optical responses to analytes, so-called long-lived luminescent probes, have been developed as probes for various biomolecules[12] including some enzymes.[13–15] Importantly, however, no such probe has yet been developed for drug-metabolizing enzymes, including NATs. Therefore, we designed the aniline-bearing complex **1** as the first turn-on luminescent probe for NAT activity (Fig. 1). For the switching function, we chose the photoinduced electron transfer (PeT) mechanism, since PeT is a widely used quenching mechanism for fluorescent molecules.[16] We previously established that intramolecular PeT can also quench lanthanide luminescence, by synthesizing and evaluating a series of complexes including **1**.[13]

We initially synthesized the probe complex **1** and the product complex **2** again to investigate their optical properties.[13] As can

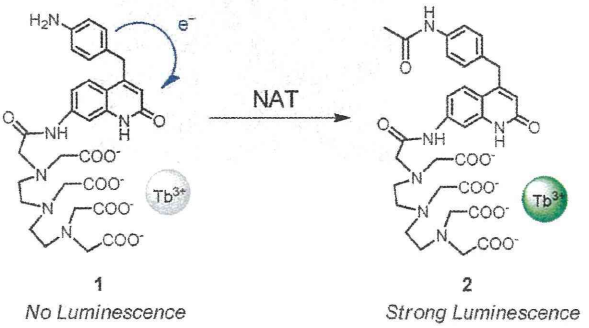


**1** *No Luminescence* **2** *Strong Luminescence*

**Fig. 1** Schematic representation of the novel NAT probe. Intraligand PeT quenching in complex **1** should be diminished by *N*-acetylation of the aniline moiety, resulting in strong green luminescence.

[a] *Graduate School of Pharmaceutical Sciences, The University of Tokyo, 7-3-1 Hongo, Bunkyo-ku, Tokyo 113-0033, Japan. E-mail: tlong@mol.f.u-tokyo.ac.jp; Fax: +81-3-5841-4855; Tel: +81-3-5841-4850*
[b] *Graduate School of Engineering, Osaka University, 2-1 Yamadaoka, Suita, Osaka 565-0871, Japan*
[c] *Graduate School of Medicine, The University of Tokyo, 7-3-1 Hongo, Bunkyo-ku, Tokyo 113-0033, Japan*
[d] *Open Innovation Center for Drug Discovery, The University of Tokyo, 7-3-1 Hongo, Bunkyo-ku, Tokyo 113-0033, Japan*

† Electronic supplementary information (ESI) available: Experimental details, photophysical properties of **1** and **2**, dependence of luminescence increase on acetyl CoA, HPLC chart of reaction mixture, results of conventional fluorescence measurement, inhibition assay, selectivity among human NATs, experiment with cell cytosols, and references. See DOI: 10.1039/c2cc17622j

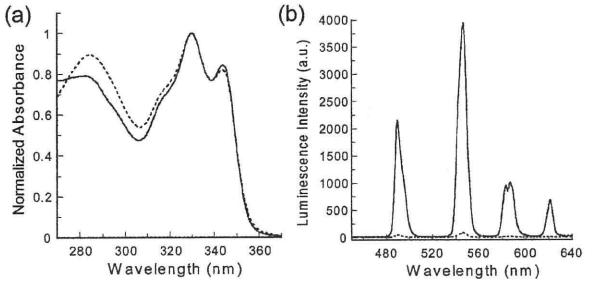


**Fig. 2** Normalized absorption (a) and luminescence (b) spectra of complexes **1** (5 μM, dashed line) and **2** (5 μM, solid line) in 100 mM Tris-HCl buffer (pH 7.4). The excitation wavelength was 325 nm.

be seen from their absorption and emission spectra (Fig. 2), they have strikingly different luminescence quantum yields (Table S1, ESI†), which can be explained by PeT from an aniline moiety. Next, we examined whether complex **1** can be *N*-acetylated by NAT. In this experiment, to allow comparison with previous reports,[7,8] we used the enzyme from pigeon liver, which was the first characterized NAT, and is considered to be representative.[17] Upon incubation of complex **1** with NAT and an acetyl CoA regenerating system in Tris-HCl buffer, a marked, time-dependent increase of green luminescence from the $Tb^{3+}$ excited state ($^5D_4$) was observed (Fig. 3). In contrast, control samples without acetyl CoA showed no luminescence increase, indicating that the increased luminescence was due to the acetylated complex **2** (Fig. S1, ESI†).[18] This was confirmed by HPLC analysis of the reaction mixture (Fig. S2, ESI†). A single peak with strong emission at 545 nm was detected, and its retention time was identical with that of complex **2**. As expected, when the time-resolved technique was not used, intrinsic fluorescence and scattering light resulted in a reduced S/N ratio of the measurement (Fig. S3, ESI†).

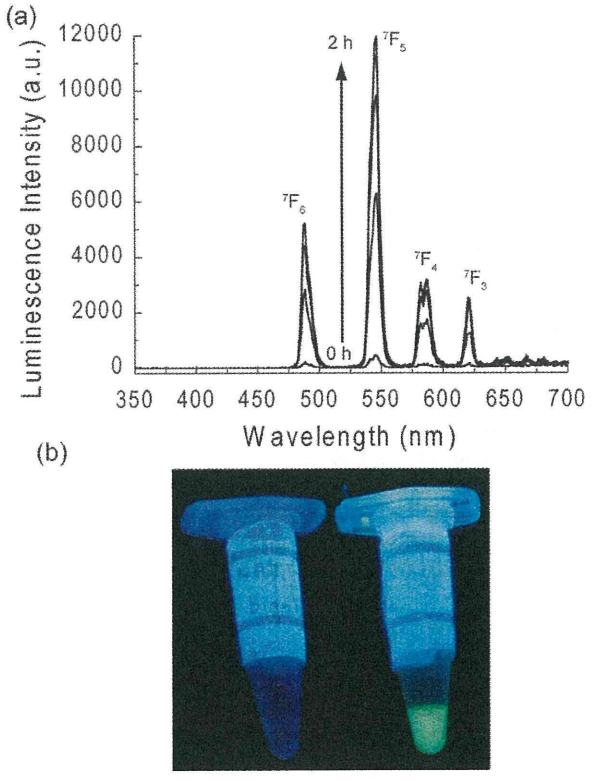


**Fig. 3** *N*-Acetylation reaction of **1** with NAT. (a) Time-resolved emission spectra of complex **1** at 0, 15, 30, 60, and 120 minutes after probe addition. NAT assay was performed at 37 °C in 0.1 M Tris-HCl buffer (pH 7.4), containing 0.2 U NAT, and 0.1 mM complex **1** (see ESI† for details). The attribution of each emission band is shown. The excitation wavelength was 340 nm. (b) Photograph of the reaction mixtures in the absence (left) and presence (right) of NAT under illumination at 312 nm.

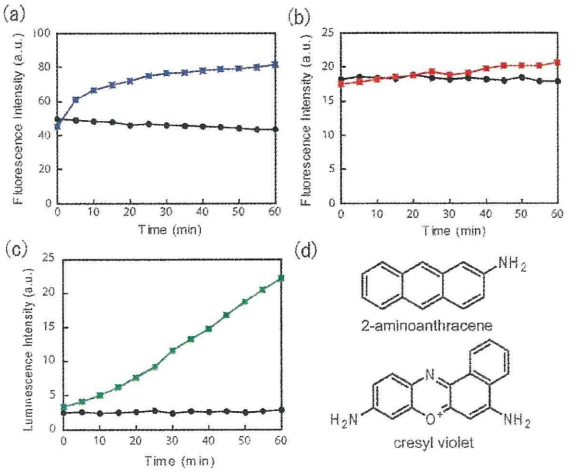


**Fig. 4** NAT activity on a 96-well microplate detected with (a) 2-aminoanthracene, (b) cresyl violet, and (c) complex **1**. Colored plots represent the data from reaction wells, and black plots represent those from control wells without acetyl CoA (for details, see ESI†). For the $Tb^{3+}$ complex **1**, time-resolved measurement was performed. Chemical structures of the fluorogenic substrates are shown in (d).

Next, the practical utility of the novel probe **1** was examined in comparison with previously reported fluorescent probes, 2-aminoanthracene[7] and cresyl violet.[8,19] For use in drug discovery research, high sensitivity and reliability of microplate assays are essential. Time-resolved luminescence measurements using lanthanide complexes are particularly favorable, because they provide extremely high S/N ratios and are not susceptible to interference from other fluorescent compounds.[13,20] As shown in Fig. 4, complex **1** exhibited a marked 10-fold increase of luminescence in time-resolved measurement at 545 nm after 60 min incubation in 96 well plates. Notably, the increase of luminescence was inhibited in the presence of quercetin (20 μM)[21] and PABA (1 mM)[3,22] (Fig. S4, ESI†). In contrast, conventional fluorescent probes showed less than 2-fold increase because of high background fluorescence from proteins and the plate (Fig. 4). These results indicate that complex **1** would be suitable for large-scale inhibitor or substrate screening.[23]

In humans, NAT2 is expressed only in specific cells including HepG2 and A549,[24] whereas NAT1 is expressed in almost all types of cells,[21,23] including HeLa.[25] Therefore, we qualitatively examined the specificity of complex **1** for NATs (Fig. S5, ESI†). The results suggest that *N*-acetylation of complex **1** is much more efficiently catalysed by NAT2 than by NAT1, *i.e.*, the probe shows high specificity for NAT2.

Finally, complex **1** was applied to the detection of endogenous NAT activity of cultured cells. We prepared cytosol

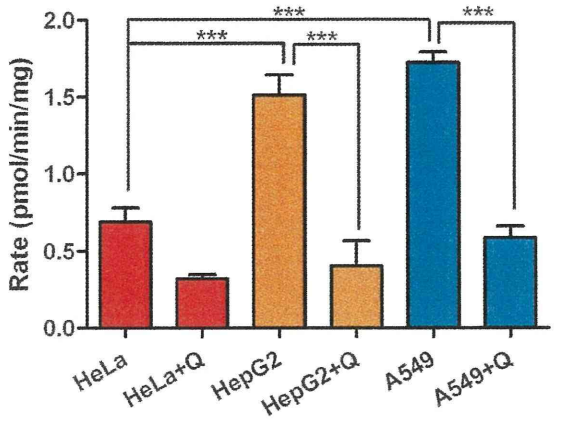


**Fig. 5** NAT activity of different cell cytosols. Shown is the increase of luminescence of the cytosol incubated with complex **1** (10 μM), or complex **1** and quercetin (denoted as Q, 10 μM). Data are shown as mean ± SEM ($n$ = 4). *** indicates $p < 0.001$ (ANOVA with Tukey's test).

from HepG2 cells, and incubated it with complex **1**. As shown in Fig. S6 (ESI†), a clear time-dependent increase of luminescence intensity was observed within 5 min, and was inhibited by quercetin (10 μM). The results indicated that the probe successfully detected endogenous NAT activity of the cells. Luminescence increase was also observed in cytosol from A549 and HeLa cells (Fig. 5), indicating that the probe can quantify NAT activity independently of the cell type.

In conclusion, we herein introduced the first long-lifetime (>1 ms) luminescent probe, complex **1**, for NATs, which utilized an intraligand PeT process as the sensing mechanism.

The synthesized probe exhibited as large as approximately 100-fold increase of luminescence after reaction with NAT. Time-resolved measurement using this probe provided a simple, sensitive, and homogeneous assay of NAT activity of purified recombinant human enzyme or cell lysate. In contrast to hydrolytic enzymes,[13,15] transferases such as NATs and kinases[14] have relatively strict substrate specificity, which often hampers the development of optical probes. In this sense, the rapid *N*-acetylation of complex **1** by human NAT2 is somewhat serendipitous and could not have been rationally predicted. Taken together, our results indicate that this probe is superior to other currently available NAT sensors. It is expected to be a useful tool for biological and pharmaceutical research, *e.g.*, to screen NAT inhibitors and substrates.

We thank Kiyoshi Sasakura, Masayo Sakabe, and Tomoya Hirata for experimental assistance, and Kenjiro Hanaoka and Toru Komatsu for helpful advice. This work was supported in part by the Ministry of Education, Culture, Sports, Science and Technology of Japan (Grant No. 22000006 to T.N., and 23651231 to T.T.), and by a grant from the New Energy and Industrial Technology Development Organization (NEDO) of Japan (to T.T.). T.T. was also supported by the Cosmetology Research Foundation, and Mochida Memorial Foundation for Medical and Pharmaceutical Research, Japan.

## Notes and references

1 (*a*) N. J. Butcher, S. Boukouvala, E. Sim and R. F. Minchin, *The Pharmacogenomics Journal*, 2002, **2**, 30; (*b*) S. Boukouvala and G. Fakis, *Drug Metab. Rev.*, 2005, **37**, 511; (*c*) I. Cascorbi, J. Brockmöller, P. M. Mrozikiewicz, A. Müller and I. Roots, *Drug Metab. Rev.*, 1999, **31**, 489.
2 (*a*) N. J. Butcher, N. L. Tetlow, C. Cheung, G. M. Broadhurst and R. F. Minchin, *Cancer Res.*, 2007, **67**, 85; (*b*) J. Dairou, N. Atmane, F. Rodrigues-Lima and J.-M. Dupret, *J. Biol. Chem.*, 2003, **279**, 7708.
3 N. J. Butcher, K. F. Ilett and R. F. Minchin, *Mol. Pharmacol.*, 2000, **57**, 468.
4 N. Atmane, J. Dairou, A. Paul, J.-M. Dupret and F. Rodrigues-Lima, *J. Biol. Chem.*, 2003, **278**, 35086.
5 M. Blum, A. Demierre, D. M. Grant, M. Heim and U. A. Meyer, *Proc. Natl. Acad. Sci. U. S. A.*, 1991, **88**, 5237.
6 (*a*) *The Molecular Probes Handbook*, ed. I. Johnson and M. T. Z. Spence, Life Technologies, Carlsbad, 11th edn, 2010; (*b*) T. Terai and T. Nagano, *Curr. Opin. Chem. Biol.*, 2008, **12**, 515.
7 L. Servillo, C. Balestrieri, M. Boccellino, M. L. Balestrieri, L. Quagliuolo and A. Giovane, *Anal. Biochem.*, 1999, **273**, 105.
8 M. Solomon and D. Stansbie, *Anal. Biochem.*, 1984, **141**, 337.
9 L. Cui, Y. Zhong, W. Zhu, Y. Xu and X. Qian, *Chem. Commun.*, 2010, **46**, 7121.
10 (*a*) E. G. Moore, A. P. S. Samuel and K. N. Raymond, *Acc. Chem. Res.*, 2009, **42**, 542; (*b*) S. V. Eliseeva and J.-C. G. Bünzli, *Chem. Soc. Rev.*, 2010, **39**, 189.
11 (*a*) M. Lee, M. S. Tremblay, S. Jockusch, N. J. Turro and D. Sames, *Org. Lett.*, 2011, **13**, 2802; (*b*) S. Mizukami, T. Yamamoto, A. Yoshimura, S. Watanabe and K. Kikuchi, *Angew. Chem., Int. Ed.*, 2011, **50**, 8750.
12 (*a*) B. Song, G. Wang, M. Tan and J. Yuan, *J. Am. Chem. Soc.*, 2006, **128**, 13442; (*b*) A. R. Lippert, T. Gschneidtner and C. J. Chang, *Chem. Commun.*, 2010, **46**, 7510; (*c*) K. Hanaoka, K. Kikuchi, H. Kojima, Y. Urano and T. Nagano, *J. Am. Chem. Soc.*, 2004, **126**, 12470; (*d*) Y. Chen, W. Guo, Z. Ye, G. Wang and J. Yuan, *Chem. Commun.*, 2011, **47**, 6266.
13 (*a*) T. Terai, K. Kikuchi, S. Iwasawa, T. Kawabe, Y. Hirata, Y. Urano and T. Nagano, *J. Am. Chem. Soc.*, 2006, **128**, 6938; (*b*) M. Kawaguchi, T. Okabe, T. Terai, K. Hanaoka, H. Kojima, I. Minegishi and T. Nagano, *Chem.–Eur. J.*, 2010, **16**, 13479.
14 M. Tremblay, M. Lee and D. Sames, *Org. Lett.*, 2008, **10**, 5.
15 M. Tremblay, M. Halim and D. Sames, *J. Am. Chem. Soc.*, 2007, **129**, 7570.
16 (*a*) Y. Urano, M. Kamiya, K. Kanda, T. Ueno, K. Hirose and T. Nagano, *J. Am. Chem. Soc.*, 2005, **127**, 4888; (*b*) T. Ueno, Y. Urano, H. Kojima and T. Nagano, *J. Am. Chem. Soc.*, 2006, **128**, 10640.
17 (*a*) I. M. Westwood, A. Kawamura, E. Fullam, A. J. Russell, S. G. Davies and E. Sim, *Curr. Top. Med. Chem.*, 2006, **6**, 1641; (*b*) H. H. Andres, H. J. Kolb and J. Weiss, *Biochim. Biophys. Acta, Protein Struct. Mol. Enzymol.*, 1983, **746**, 182.
18 We confirmed in a separate experiment that another control mixture without NAT showed no increase of luminescence at all.
19 Amonafide (ref. 9) was not examined because it is not commercially available from major reagent companies.
20 (*a*) I. Hemmilá and V.-M. Mukkala, *Crit. Rev. Clin. Lab. Sci.*, 2001, **38**, 441; (*b*) J. Yuan and G. Wang, *TrAC, Trends Anal. Chem.*, 2006, **25**, 490.
21 V. Kukongviriyapan, N. Phromsopha, W. Tassaneeyakul, U. Kukongviriyapan, B. Sripa, V. Hahnvajanawong and V. Bhudhisawasdi, *Xenobiotica*, 2006, **36**, 15.
22 This compound works as a competitive substrate, thereby decelerating the catalysis of complex **1**.
23 A. J. Russell, I. M. Westwood, M. H. J. Crawford, J. Robinson, A. Kawamura, C. Redfield, N. Laurieri, E. D. Lowe, S. G. Davies and E. Sim, *Bioorg. Med. Chem.*, 2009, **17**, 905.
24 A. Husain, X. Zhang, M. A. Doll, J. C. States, D. F. Barker and D. W. Hein, *Drug Metab. Dispos.*, 2007, **35**, 721.
25 L. Liu, C. R. Wagner and P. E. Hanna, *Chem. Res. Toxicol.*, 2008, **21**, 2005.

JACS
JOURNAL OF THE AMERICAN CHEMICAL SOCIETY

Article

pubs.acs.org/JACS

# No-Wash Protein Labeling with Designed Fluorogenic Probes and Application to Real-Time Pulse-Chase Analysis

Shin Mizukami,[†,‡] Shuji Watanabe,[†] Yuri Akimoto,[†] and Kazuya Kikuchi*[,†,‡]

[†]Division of Advanced Science and Biotechnology, Graduate School of Engineering, Osaka University, 2-1 Yamadaoka, Suita, Osaka 565-0871, Japan

[‡]Immunology Frontier Research Center (IFReC), Osaka University, 3-1 Yamadaoka, Suita, Osaka 565-0871, Japan

*Web-Enhanced Feature* *Supporting Information*

**ABSTRACT:** Small molecule labeling techniques for cellular proteins under physiological conditions are very promising for revealing new biological functions. We developed a no-wash fluorogenic labeling system by exploiting fluorescence resonance energy transfer (FRET)-based fluorescein-cephalosporin-azopyridinium probes and a mutant $\beta$-lactamase tag. Fast quencher elimination, hydrophilicity, and high resistance against autodegradation were achieved by rational refinement of the structure. By applying the probe to real-time pulse-chase analysis, the trafficking of epidermal growth factor receptors between cell surface and intracellular region was imaged. In addition, membrane-permeable derivatization of the probe enabled no-wash fluorogenic labeling of intracellular proteins.

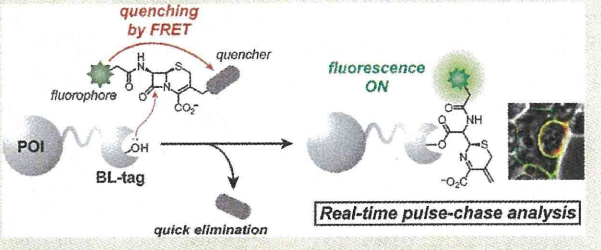


## INTRODUCTION

By imaging protein dynamics, valuable information about target proteins can be obtained, such as their intracellular localization, expression and degradation timings, and interactions with other proteins. Fluorescent proteins (FPs) have been utilized for this purpose because advances in fluorescence microscopy have enabled the real-time visualization of target proteins genetically fused with FPs in living cells.[1] Combining the use of FPs with probe design strategies based on fluorescence resonance energy transfer (FRET) has also led to the production of innovative probes for biological studies.[2] However, such genetic engineering approaches have critical limitations. For instance, we cannot label target proteins expressing at specific timings by using FPs. Although imaging the dynamics of cell cycle progression was achieved by exploiting the cell-cycle dependent proteolysis of two FP-labeled ubiquitination oscillators,[3] the strategy cannot be generally applied to other dynamic biological processes. In addition, organic or inorganic chemistry-based synthetic molecules provide a wider range of functions. Therefore, techniques for labeling cellular proteins with synthetic molecules under physiological conditions are obviously useful and promising in revealing new biological functions.

Many research groups have reported tag-based protein labeling techniques, in which the target proteins are genetically fused with a peptide tag or a small-protein tag.[4] These tags are specifically modified with the corresponding small-molecule probes by a chemical or enzyme reaction, coordination, protein−ligand interaction, etc. By using such labeling technologies, proteins expressed at specific timings can be visualized. However, most labeling techniques, except the tetracysteine-tag technology,[4a] do not exhibit a fluorogenic property. In other words, the washout of the unlabeled probes is required prior to microscopic imaging. Tetracysteine-tag technology also requires the washing procedure for imaging with a high signal/noise ratio to avoid nonspecific labeling.[5] Because the washout procedure takes at least 15 min, precise pulse-chase experiments with shorter time intervals are practically impossible with conventional labeling technologies. In addition, the complete washout of the unreacted probes inside cells is difficult, because synthetic probes often accumulate in various organelles.

We developed a fluorogenic protein labeling system that exploits a mutant of 29-kDa TEM-1 $\beta$-lactamase (BL-tag) and the synthetic $\beta$-lactam probes.[6] This technology is quite versatile, and various applications such as multicolor fluorescence imaging,[7] a pulse-chase experiment with luminescent quantum dots via specific biotinylation,[8] and time-resolved protein imaging with a lanthanide-based probe[9] have been demonstrated. In addition, the use of FRET-based labeling probes[6] in this system conferred both specificity and a turn-on fluorescence property. The labeling mechanism involves two steps: an initial noncatalytic enzyme reaction and subsequent quencher elimination via a self-immolative reaction (Scheme 1).

Effective FRET quenching of the probes and fluorescence recovery after *in vitro* protein labeling via a self-immolative reaction have been observed. However, the no-wash labeling of live-cell proteins has not been performed because of a slow turn-on fluorescence response. In addition, the high hydro-

**Received:** September 2, 2011
**Published:** January 6, 2012





dx.doi.org/10.1021/ja208290f | J. Am. Chem.Soc. 2012, 134, 1623−1629

**Scheme 1. Schematic Illustration of Fluorogenic Protein Labeling Mechanism Using Previous and New Probes Based on Fluorescence Resonance Energy Transfer (FRET)[a]**

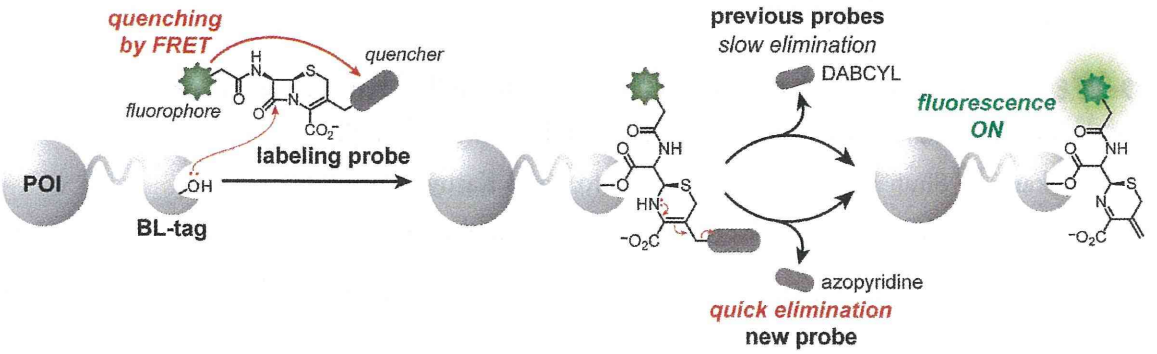


[a]POI: protein of interest.

**Chart 1. Structures of Synthesized Compounds**

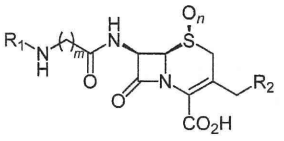

| | $R_1$ | $R_2$ | $m$ | $n$ |
|---|---|---|---|---|
| CCD | 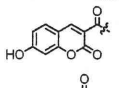 | 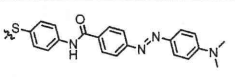 | 1 | 0 |
| FCD | 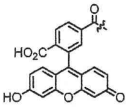 | 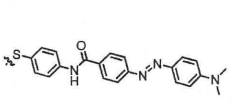 | 1 | 0 |
| RCD | 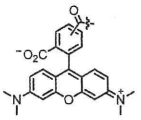 | 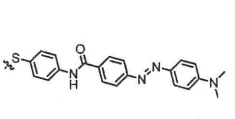 | 1 | 0 |

| | $R_1$ | $R_2$ | $m$ | $n$ |
|---|---|---|---|---|
| CAP1 | H | 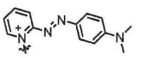 | 1 | 0 |
| CAP2 | H | 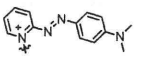 | 2 | 0 |
| FCAP2 | 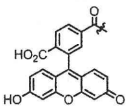 | 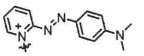 | 2 | 0 |
| FCAPO2 | 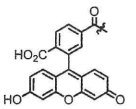 | 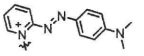 | 2 | 1 |
| FCAPO2-DA | 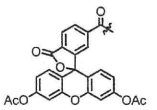 | 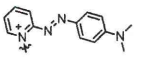 | 2 | 1 |

phobicity of the probes, mainly of the DABCYL group, caused a tendency to accumulate in the hydrophobic regions of cells such as plasma membranes, although nonspecific accumulation disappeared after washing the cells. When analyzing the quick dynamics of target proteins using pulse-chase experiments, the labeling rate should be as high as possible. Thus, it is very important to develop superior labeling probes that exhibit a quick turn-on fluorescence response and thus enable real-time pulse-chase experiments without the washing procedure. However, no such probes have been reported thus far.

Herein, we report the rational development of a novel probe that can exhibit a fast fluorogenic labeling response for BL-tag technology. The probe did not require the washing procedure in live cell imaging and thus provided an innovative protein analytical method using real-time pulse-chase analysis. In addition, the membrane-permeable derivatization of the probe by the esterification enabled the no-wash fluorogenic labeling of intracellular proteins.

## RESULTS

**Design, Synthesis, And Photophysical and Biochemical Properties of Novel Labeling Probes.** We investigated the optimization of the leaving quencher for no-wash fluorogenic labeling. As described above, the fluorogenic labeling process is divided into two steps: namely, enzymatic labeling and subsequent elimination reaction. Preliminary absorption analysis of the synthesized labeling probes showed that the nucleophilic enzyme reaction proceeds quickly and the following elimination is the rate-determining step. Elimination rates generally depend on the elimination ability of the leaving groups, which is correlated with the $pK_a$ value of the conjugate acid. The $pK_a$ of the thiophenol group of FCD (Chart 1) was estimated to be about 6.5,[10] and it was thus expected that a decrease in $pK_a$ would accelerate the elimination rate. It has been reported that azopyridinium-conjugated cephalosporin induces fast elimination from the 3′-position after hydrolysis of $\beta$-lactam, because the corresponding conjugate acid has a lower $pK_a$ (4.3).[11] Because of its fast elimination, hydrophilicity, and absorption spectra, we chose 2-(4-dimethylaminophenylazo)-pyridinium as the quencher. Although this azopyridinium compound is not widely known as a FRET quencher, as compared with DABCYL, the absorption spectral property from 450 to 600 nm fulfills the requirement for quenching green or orange fluorescence of fluorescein or tetramethylrhodamine, respectively. In addition, the hydrophilicity of


dx.doi.org/10.1021/ja208290f | J. Am. Chem.Soc. 2012, 134, 1623–1629

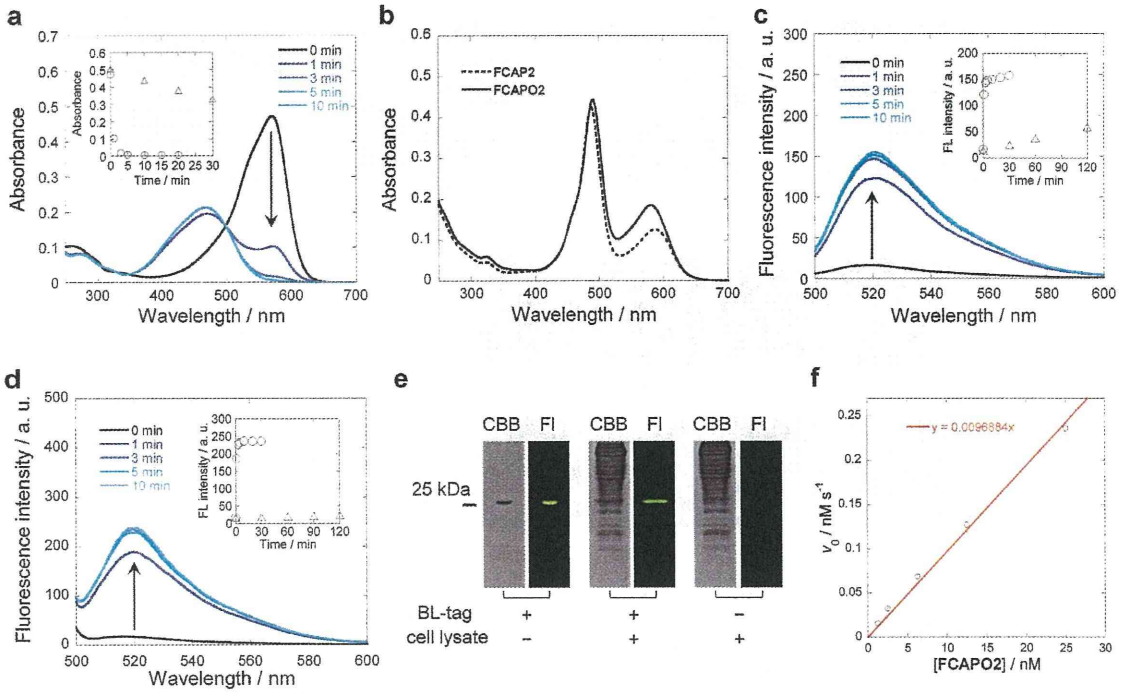


**Figure 1.** Spectral and protein labeling properties of synthesized probes. All reactions were performed in 100 mM HEPES buffer (pH 7.4) at 25 °C. (a) Time-dependent absorption spectra of 10 $\mu$M CAP1, obtained by incubation with 40 nM WT TEM. (inset) Time-dependent absorbance ($\lambda$ = 570 nm) of CAP1 with (circle) or without (triangle) WT TEM. (b) Absorption spectra of 5 $\mu$M FCAP2 (dotted line) and 5 $\mu$M FCAPO2 (solid line). (c, d) Time-dependent emission spectra of 500 nM FCAP2 (c, $\lambda_{ex}$ = 487 nm) or 500 nM FCAPO2 (d, $\lambda_{ex}$ = 490 nm), obtained by incubation with 1 $\mu$M BL-tag. (inset) Time-dependent fluorescence intensity of 500 nM FCAP2 (c, $\lambda_{ex}$ = 487 nm, $\lambda_{em}$ = 518 nm) or 500 nM FCAPO2 (d, $\lambda_{ex}$ = 490 nm, $\lambda_{em}$ = 518 nm) with (circle) or without (triangle) BL-tag. (e) Electrophoresis gel images of BL-tag incubated with FCAPO2 in the presence or absence of HEK293T cell lysate. CBB: Coomassie Brilliant Blue staining. Fl: fluorescence. (f) Plot of initial labeling reaction rate $v_0$ versus probe concentration [FCAPO2]. [BL-tag] = 125 nM.

azopyridinium (calculated logP = −1.9) was expected to enhance the practical utility in live cell imaging.

We designed and synthesized CAP1 (Chart 1 and Scheme S1, Supporting Information) as the key compound, which can be conjugated with various fluorophores, to develop novel fluorogenic probes. The elimination reaction rate of CAP1 was investigated using wild-type TEM-1 $\beta$-lactamase (WT TEM). The absorption maximum of CAP1 in HEPES buffer (pH 7.4) was observed at 580 nm, and the peak quickly decreased by the addition of WT TEM (Figure 1a). This spectral change indicates that azopyridinium was eliminated, getting converted into the neutral azopyridine form.[11a] However, the absorption spectrum of CAP1 gradually changed in an enzyme-free buffer solution (Figure 3a inset), probably because CAP1 degraded automatically in neutral aqueous solution. This degradation was also observed in dimethyl sulfoxide (DMSO)-$d_6$. Furthermore, fluorophore conjugation to the amino group was unsuccessful because of the instability of CAP1. We suspected that the instability might be caused by intramolecular aminolysis via the six-membered ring formation (Scheme S2, Supporting Information).

To avoid the intramolecular cyclization, we designed an improved synthetic scheme (Scheme S3, Supporting Information) via CAP2 (Chart 1), which has an aminoethyl group instead of the aminomethyl group of CAP1. As a result, CAP2 showed good stability in solution. CAP2 showed equally quick absorption spectral change by the addition of WT TEM as CAP1 (Figure S1a, Supporting Information). CAP2 also showed enough stability in neutral buffer solution (Figure S1b, Supporting Information). Thus, the intramolecular cyclization observed in the case of CAP1 could be completely suppressed by linker elongation in CAP2.

A new fluorescent probe, FCAP2 (Chart 1), was successfully synthesized from CAP2 (Scheme S3, Supporting Information). FCAP2 showed the absorption maxima at 487 nm ($\lambda$ = 85 000 M$^{-1}$ cm$^{-1}$) and 589 nm ($\varepsilon$ = 25 200 M$^{-1}$ cm$^{-1}$) for fluorescein and azopyridinium, respectively (Figure 1b, dotted line). As expected, the fluorescence of FCAP2 was largely quenched ($\Phi$ = 0.03) by FRET and recovered by incubation with BL-tag protein (Figure 1c). The fluorescence increase, as well as the absorption spectral change, was very quick and completed within a few minutes (Figure 1c inset, circle). This indicates the great potential of FCAP2 in real-time fluorescence imaging. However, the fluorescence of FCAP2 was unexpectedly increased in the absence of BL-tag, probably as a result of autohydrolysis (Figure 1c inset, triangle).

A previous report has suggested that stability of cephalosporin derivatives is improved by oxidizing the sulfides of cephalosporins to sulfoxides.[12] Therefore, FCAPO2 (Chart 1), the oxidized compound of FCAP2, was designed and synthesized (Scheme S4). FCAPO2 showed an absorption spectrum very similar to that of FCAP2, with two peaks for fluorescein ($\lambda$ = 490 nm, $\varepsilon$ = 89 000 M$^{-1}$ cm$^{-1}$) and azopyridinium ($\lambda$ = 581 nm, $\varepsilon$ = 37 000 M$^{-1}$ cm$^{-1}$) (Figure 1b, solid line). The fluorescence of FCAPO2 was largely quenched ($\Phi$ = 0.02) by FRET and quickly recovered by


dx.doi.org/10.1021/ja208290f | J. Am. Chem.Soc. 2012, 134, 1623–1629

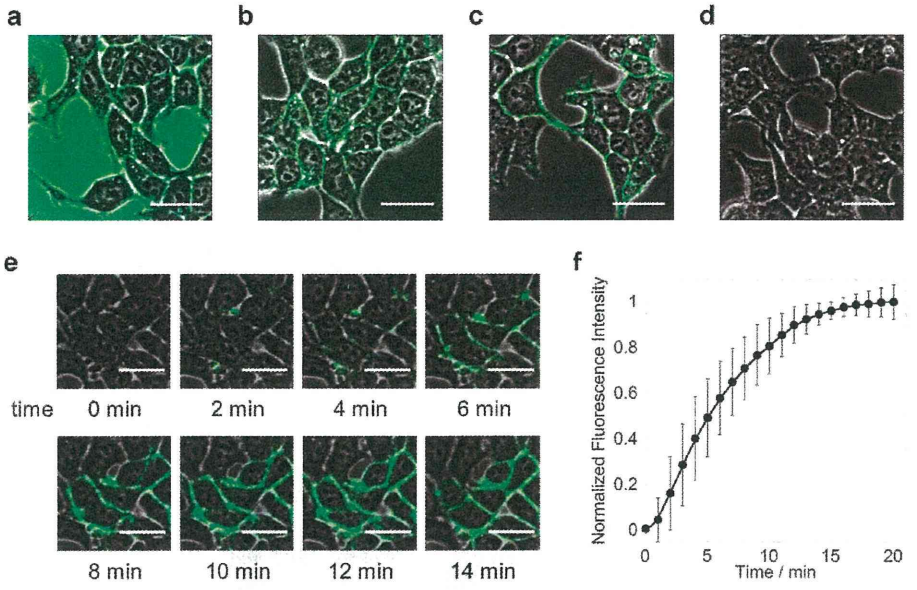


**Figure 2.** No-wash fluorogenic labeling of cell surface proteins. (a–d) HEK293T cells expressing BL-EGFR (a–c) or EGFR (d) were treated with 500 nM FA (a,b) or FCAPO2 (c,d) at 37 °C. Fluorescence images ($\lambda_{ex}$ = 473 nm) were captured using a confocal fluorescence microscope without (a, c, d) or with (b) the washing procedure. (e, f) Time-lapse fluorogenic labeling of cell surface BL-EGFR with 10 nM FCAPO2 at 37 °C. Time-course graph of the fluorescence images (e) and the averaged fluorescence intensity for the complete field of view ($n$ = 4) (f). Scale bar: 20 $\mu$m. See also Movie 1 in the HTML version of this paper.

incubation with BL-tag protein (Figure 1d). The fluorogenic labeling and elimination reactions were very quick and completed within a few minutes (Figure 1d inset, circle). The stability of FCAPO2 in neutral aqueous solution was considerably increased, as compared with that of FCAP2 (Figure 1d inset, triangle) and was considered enough for practical use in physiological studies. With regard to specificity, FCAPO2 labeled only BL-tag, even in the presence of HEK293T cell lysate (Figure 1e). All these results indicate that we successfully developed a highly stable labeling probe that showed quick fluorogenic response after specific protein labeling.

Then, the precise labeling kinetics of FCAPO2 toward BL-tag was studied. To a solution of the excess tag protein (125 nM), 1.25–25 nM FCAPO2 was added, and the initial reaction rate calculated from the fluorescence increase (Figure S4, Supporting Information) was plotted against the probe concentration (Figure 1f). As a result, the bimolecular labeling rate constant was determined to be $7.8 \times 10^4$ $M^{-1}$ $s^{-1}$. This value indicates that the combination of FCAPO2 and BL-tag is the fastest fluorogenic labeling system among the highly selective labeling technologies, as shown in Table S1 in the Supporting Information.

**Fluorogenic Labeling of Cell Surface Proteins with FCAPO2.** Fluorogenic labeling of cell surface proteins with FCAPO2 was examined using living cells. BL-tag-fused epidermal growth factor receptor (BL-EGFR) proteins were expressed in HEK293T cells, following treatment with FCAPO2 or nonfluorogenic FA (Figure S2a, Supporting Information) at a concentration of 500 nM. After 10 min of incubation, the cells were observed with a confocal fluorescence microscope without washout of the probe. In the case of FA, high background fluorescence signals were observed in the medium (Figure 2a), although the fluorescence labeling of the membrane proteins was visible after the washing procedure (Figure 2b), as previously reported.[7] On the other hand, when the cells were incubated with FCAPO2, green fluorescence increased along the plasma membranes within a few minutes without the washing procedure (Figure 2c). This fluorescence increase was not observed in the cells expressing EGFR without BL-tag (Figure 2d).

Next, we performed time-lapse imaging of protein labeling with FCAPO2. Under confocal fluorescence microscopy, 10 nM FCAPO2 was added to HEK293T cells expressing BL-EGFR. Consecutive capture of cell images without the washing procedure showed time-dependent fluorescence enhancement along the plasma membranes (Figure 2e and Movie 1). The fluorogenic labeling rate of the living cell surface proteins was investigated in time-lapse fluorescence images. Even with highly diluted probe ([FCAPO2] = 10 nM), the labeling rate was fast and labeling was almost completed within 15 min (Figure 2f). Based on the results of these *in vitro* and live cell experiments, we conclude that this new labeling system is faster than previously reported fluorogenic labeling systems, including our previous reports and the SNAP-tag-based fluorogenic labeling system reported.[13]

**Real-Time Imaging of Cell Surface Expression and Internalization of Target Proteins by Using Dual Probes.** Although imaging of protein trafficking is one of the promising applications of protein labeling techniques, the washing procedures in the current technologies restrict wide application of the techniques. Therefore, we performed real-time pulse-chase analysis of protein expression on cell surface by using FCAPO2. As pulse-chase analysis visualizes target protein expression at a specific time, quick protein labeling that does not require the washing procedure would be very effective for pulse-chase analysis of protein trafficking with high temporal resolution.

We constructed a protein analytical method, in which internalization of cell surface proteins and cell surface

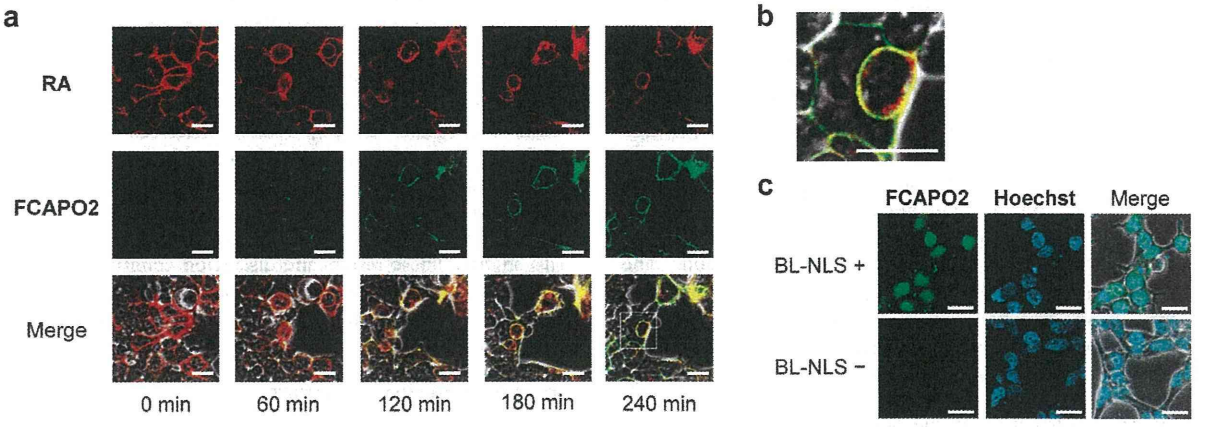


**Figure 3.** Real-time pulse-chase analysis and no-wash fluorogenic labeling of intracellular proteins. (a, b) Real-time fluorescence imaging of BL-EGFR trafficking by using FCAPO2 and RA. HEK293T cells were labeled with 100 nM RA prior to incubation with 20 nM FCAPO2 at 37 °C. (a) (top row) Fluorescence images ($\lambda_{ex}$ = 559 nm) for RA, (middle row) fluorescence images ($\lambda_{ex}$ = 473 nm) for FCAPO2, (bottom row) merged images of fluorescence and phase contrast microscopy. (b) Magnified image of the square marked in the bottom row in part a. (c) Intracellular protein labeling with FCAPO2-DA ($\lambda_{ex}$ = 473 nm). HEK293T cells expressing BL-NLS (top) and nontransfected cells (bottom) were incubated with 5 $\mu$M FCAPO2-DA and 100 ng mL$^{-1}$ Hoechst33342 at 37 °C for 2 h. Scale bar: 20 $\mu$m.

expression of genetically identical proteins can be discriminatively visualized. In the protocol, BL-EGFR proteins displayed on the cell surface were labeled in advance with a membrane-impermeable rhodamine probe, RA (Figure S2b, Supporting Information). After the culture medium was replaced with a fresh medium, FCAPO2 was added, and cell images were captured using a confocal fluorescence microscope (Figure 3a and b). Initially, only the red fluorescence of RA was detected around the plasma membranes. Thereafter, the red fluorescence signals gradually internalized and formed bright spots in the cells in a time-dependent manner. This trafficking indicates the endocytosis of EGFR caused by the stimulation of epidermal growth factor (EGF) included in the serum. On the other hand, the green fluorescence of FCAPO2 was scarcely observed in the beginning. However, the green fluorescence signals gradually increased along the plasma membranes, probably due to the fluorogenic labeling of newly expressed proteins on the cell surface. These results suggest that this imaging methodology can discriminately visualize EGFR trafficking from the cell surface to the intracellular region, as well as in the opposite direction.

**Fluorogenic Labeling of Intracellular Proteins with the Cell-Permeable Probe FCAPO2-DA.** We developed cell-permeable labeling probes for intracellular proteins by utilizing bacampicillin, which is a clinical penicillin-type $\beta$-lactam prodrug developed for improving intestinal absorption.[14] However, these probes do not have fluorogenic property because it is very difficult to incorporate leaving groups in the bacampicillin structure. Therefore, we extended the probe design of FCAPO2 to achieve fluorogenic labeling of intracellular proteins. FCAPO2 has three anionic groups and one cationic group in its structure. Of the three anionic groups, two are in the fluorescein structure, and the remaining anionic carboxylate and the cationic group are in cephalosporin and azopyridinium, respectively. Because the latter two groups are very close, they are likely to form an intramolecular ion pair. Hence, we hypothesized that the protection of only two anionic groups in fluorescein in FCAPO2 might enable probe introduction into living cells, although previous reports suggest that the carboxylate of cephalosporin-based probes needs to be protected to permeate living cell membranes.[15]

We acetylated FCAPO2 to obtain FCAPO2-DA (Chart 1 and Scheme S5 in the Supporting Information). The absorption spectra of FCAPO2-DA indicated that it was quickly hydrolyzed by WT TEM (Figure S3a, Supporting Information), although it was considerably stable for several hours in aqueous solution (Figure S3b, Supporting Information). FCAPO2-DA showed no fluorescence (Figure S3c, Supporting Information), similar to the other diacetylated fluorescein derivatives.[16]

To assess the intracellular labeling property of FCAPO2-DA, we used a BL-tag protein that localizes in cell nuclei, BL-tag-fused nuclear localization signal (BL-NLS).[14] BL-NLS has three consecutive simian virus 40 (SV40) large T antigen NLS at the C terminus of BL-tag. HEK293T cells expressing BL-NLS were incubated with FCAPO2-DA, and the cell permeability and the fluorogenic labeling property of FCAPO2-DA were confirmed by confocal fluorescence microscopy. As expected, FCAPO2-DA exhibited cell permeability, and the fluorescence gradually accumulated at the cell nuclei (Figure 3c top). No noteworthy fluorescence accumulation was detected in the nuclei of the control cells transfected with empty vector plasmids (Figure 3c bottom), even though a slight fluorescence increase was observed in whole cells, which is now under investigation. As a result, we finally developed a cell-permeable fluorogenic probe to label intracellular proteins. This probe, FCAPO2-DA, enabled no-wash intracellular protein labeling, as in the case of extracellular protein labeling with FCAPO2.

## ■ DISCUSSION

The key problem in developing a practical fluorogenic protein labeling technology by extending our previous strategy[6] was the slow quencher elimination after labeling. In principle, elimination reaction rate is correlated with the p$K_a$ of the conjugate acid of the leaving group. The p$K_a$ of 2-(4-dimethylaminophenylazo)pyridinium, which is the conjugate acid of the leaving group in FCAPO2, is 4.3.[10] This value is much smaller than that of thiophenol, which is the leaving group in our previous probes such as CCD and FCD. The fast turn-on fluorescence property of FCAP2 indicates that the p$K_a$


dx.doi.org/10.1021/ja208290f | J. Am. Chem.Soc. 2012, 134, 1623–1629

of the leaving quencher was indeed an important factor for the probe design strategy. However, the fast elimination step induced undesirable autodegradation of FCAP2. This instability was overcome by oxidizing the sulfur atom in the design of FCAPO2. In addition, the linker length between the fluorophore and the β-lactam was optimized to achieve high synthetic yields.

Another essence of the probe design is the physical properties of the leaving quencher. The quencher in FCAPO2 is the cationic azopyridinium form, and it converts into the neutral azopyridine form after elimination. The absorption spectrum of the azopyridinium shows the maximum at 581 nm and broadly ranges from 500 to 600 nm. Thus, this compound works as an efficient quencher for fluorescein. This wavelength region is also suitable for the quenching of orange to light-red fluorescent dyes such as rhodamines. Although DABCYL is often used as the quencher in many quenching FRET-based probes,[17] the shorter-wavelength absorption ($\lambda_{max}$ = 462 nm) restricts its application to red fluorescent dyes. The higher molar extinction coefficient of the azopyridinium ($\varepsilon$ = 37 000 $M^{-1}$ $cm^{-1}$) than that of DABCYL ($\varepsilon$ = 25 500 $M^{-1}$ $cm^{-1}$)[7] also confirms its utility in quenching FRET applications. Hydrophilicity of azopyridinium provides another practical advantage in biological experiments. In live cell imaging, hydrophobic probes often cause localization at membranes or subcellular organelles. With regard to this point, FCAPO2 including azopyridinium showed less accumulative properties, as compared with DABCYL-based probes. In addition, the cationic aromatic heterocycle may compensate the anionic charge of the adjacent carboxy group in cephalosporin by forming an inner salt, because FCAPO2-DA permeates living cells without the protection of the carboxylate in cephalosporin.

In widely used protocols for other protein labeling techniques, at least 15-min incubation with the probes and subsequent washing procedure are required.[18] Such procedures restrict temporal resolution and diverse experimental designs. In this study, we achieved real-time pulse-chase analysis, and discriminatively visualized the internalization of cell surface-displayed proteins and the translocation of newly expressed proteins to plasma membranes. This innovative real-time imaging provided the information about how fast protein expression occurs on the plasma membranes and how fast the proteins enter the cells. Conventional methods using FPs cannot afford to discriminate proteins that have the same amino acid sequence but different functions or history. Urano et al. and Correa, Jr. et al. separately reported similar real-time fluorogenic labeling probes based on SNAP-tag technology.[13,19] However, our BL-tag-based system with FCAPO2 exhibited much faster labeling kinetics (Table S1, Supporting Information) and requires a lower probe concentration.

## ■ CONCLUSION

In conclusion, we developed second-generation fluorogenic labeling probes by exploiting an azopyridinium compound as the leaving quencher. By rational optimization of the probe structures, we reached the design of FCAPO2, which specifically labeled BL-tag proteins and very quickly recovered its fluorescence. In a detailed kinetic study of fluorogenic labeling, the bimolecular reaction rate was the highest among the known selective and fluorogenic protein labeling methods. The outstanding properties of FCAPO2 provided a versatile cell surface protein labeling system that does not require any washing procedure. In addition, membrane-permeable derivatization of FCAPO2 to FCAPO2-DA enabled no-wash fluorogenic labeling of intracellular proteins. No-wash fluorogenic labeling for intracellular proteins is very rare, although we have developed an alternative no-wash labeling method by using highly diluted prodrug-based β-lactam probes.[14] Our no-wash fluorogenic labeling system described herein would evidently be an innovative technique that provides various applications in cell biology, one of which is described in this paper. Moreover, the fluorophore can be extended to near-infrared (NIR) fluorescent dyes, which are more suitable for *in vivo* studies. These results and discussion confirm the practical utility and promise of the mutant β-lactamase-tag-based protein labeling technology in biological studies, especially those on protein trafficking, gene expression, protein degradation, etc.

## ■ ASSOCIATED CONTENT

### Ⓢ Supporting Information

Materials, instruments, synthesis and characterization of compounds, experimental procedures, and supplementary figures and schemes. This material is available free of charge via the Internet at http://pubs.acs.org.

### Ⓦ Web-Enhanced Features

Movie 1, showing fluorogenic labeling of cell surface BL-EGFR with 10 nM FCAPO2 at 37 °C over 20 min, is available in the HTML version of this paper.

## ■ AUTHOR INFORMATION

### Corresponding Author

kkikuchi@mls.eng.osaka-u.ac.jp

## ■ ACKNOWLEDGMENTS

This work was supported by the Japan Society for the Promotion of Science (JSPS) through its Funding Program for World-Leading Innovative R&D on Science and Technology (FIRST Program), the Grant-in-Aid for Scientific Research from the Ministry of Education, Culture, Sports, Science, and Technology (MEXT) of Japan, by the CREST funding program from the Japan Science and Technology Agency (JST), and by the Grant-in-Aid from the Ministry of Health, Labor, and Welfare (MHLW) of Japan. K.K. is thankful for support from the Takeda Science Foundation and from the Naito Foundation. S.M. is thankful for support from Inamori Foundation and from Sumitomo Foundation. K.K. and S.M. are thankful for support from Asahi Glass Foundation. S.W. is thankful for support from a Global COE Fellowship of Osaka University and a JSPS Research Fellowship.

## ■ REFERENCES

(1) Chudakov, D. M.; Lukyanov, S.; Lukyanov, K. A. *Trends Biotechnol.* **2005**, *23*, 605–613.

(2) Truong, K.; Ikura, M. *Curr. Opin. Struct. Biol.* **2001**, *11*, 573–578.

(3) Sakaue-Sawano, A.; Kurokawa, H.; Morimura, T.; Hanyu, A.; Hama, H.; Osawa, H.; Kashiwagi, S.; Fukami, K.; Miyata, T.; Miyoshi, H.; Imamura, T.; Ogawa, M.; Masai, H.; Miyawaki, A. *Cell* **2008**, *132*, 487–498.

(4) (a) Griffin, B. A.; Adams, S. R.; Tsien, R. Y. *Science* **1998**, *281*, 269–272. (b) Keppler, A.; Gendreizig, S.; Gronemeyer, T.; Pick, H.; Vogel, H.; Johnsson, K. *Nat. Biotechnol.* **2003**, *21*, 86–89. (c) Chen, I.; Howarth, M.; Lin, W.; Ting, A. Y. *Nat. Methods* **2005**, *2*, 99–104. (d) Yin, J.; Liu, F.; Li, X.; Walsh, C. T. *J. Am. Chem. Soc.* **2004**, *126*, 7754–7755. (e) O'Hare, H. M.; Johnsson, K.; Gautier, A. *Curr. Opin. Struct. Biol.* **2007**, *17*, 488–494. (f) Hinner, M. K.; Johnsson, K. *Curr. Opin. Biotechnol.* **2010**, *21*, 766–776. (g) Rabuka., D. *Curr. Opin.*

*Chem. Biol.* **2010**, *14*, 790–796. (h) Sunbul, M.; Yin, J. *Org. Biomol. Chem.* **2009**, *7*, 3361–3371.
(5) (a) Stroffekova, K.; Proenza, C.; Beam, K. G. *Pfluegers Arch.* **2001**, *442*, 859–886. (b) Machleidt, T.; Robers, M.; Hanson, G. T. *Methods in Molecular Biology*; Humana Press: Totowa, 2007; Vol. *356*, pp 209–220.
(6) Mizukami, S.; Watanabe, S.; Hori, Y.; Kikuchi, K. *J. Am. Chem. Soc.* **2009**, *131*, 5016–5017.
(7) Watanabe, S.; Mizukami, S.; Hori, Y.; Kikuchi, K. *Bioconjug. Chem.* **2010**, *21*, 2320–2326.
(8) Yoshimura, A.; Mizukami, S.; Hori, Y.; Watanabe, S.; Kikuchi, K. *ChemBioChem* **2011**, *12*, 1031–1034.
(9) Mizukami, S.; Yamamoto, T.; Yoshimura, A.; Watanabe, S.; Kikuchi, K. *Angew. Chem., Int. Ed.* **2011**, *50*, 8750–8752.
(10) Dean, J. A. *Lange's Handbook of Chemistry*, 14th ed.; McGraw-Hill: New York, 1972.
(11) (a) Jones, R. N.; Wilson, H. W.; Novick, W. J. *J. Clin. Microbiol.* **1982**, *15*, 677–683. (b) Faraci, W. S.; Pratt, R. F. *J. Am. Chem. Soc.* **1984**, *75*, 1489–1490.
(12) Gao, W.; Xing, B.; Tsien, R. Y.; Rao, J. *J. Am. Chem. Soc.* **2003**, *125*, 11146–11147.
(13) Komatsu, T.; Johnsson, K.; Okuno, H.; Bito, H.; Inoue, T.; Nagano, T.; Urano, Y. *J. Am. Chem. Soc.* **2011**, *133*, 6745–6751.
(14) Watanabe, S.; Mizukami, S.; Akimoto, Y.; Hori, Y.; Kikuchi, K. *Chem.—Eur. J.* **2011**, *17*, 8342–8349.
(15) Zlokarnik, G.; Negulescu, P. A.; Knapp, T. E.; Mere, L.; Burres, N.; Feng, L.; Whitney, M.; Roemer, K.; Tsien, R. Y. *Science* **1998**, *279*, 84–88.
(16) Takakusa, H.; Kikuchi, K.; Urano, Y.; Kojima, H.; Nagano, T. *Chem.—Eur. J.* **2003**, *9*, 1479–1485.
(17) Marras, S. A. E. *Mol. Biotechnol.* **2008**, *38*, 247–255.
(18) *HaloTag Technology: Focus on Imaging*, Technical Manual; Promega: U.S.A., 2009; Available online: http://www.promega.com/.
(19) Sun, X.; Zhang, A.; Baker, B.; Sun, L.; Howard, A.; Buswell, J.; Maurel, D.; Masharina, A.; Johnsson, K.; Noren, C. J.; Xu, M. Q.; Correa, I. R. *ChemBioChem.* **2011**, *12*, 2217–2226.

DOI: 10.1002/anie.201200867

Fluorescent Probes

# Development of Protein-Labeling Probes with a Redesigned Fluorogenic Switch Based on Intramolecular Association for No-wash Live-Cell Imaging**

*Yuichiro Hori, Kyohei Nakaki, Motoki Sato, Shin Mizukami, and Kazuya Kikuchi**

Fluorescence labeling of proteins is a powerful technique for studying precise protein localization and movement in living cells. Currently, fluorescent proteins (FPs) are the primary tools in this field owing to their technical feasibility and convenience.[1,2] Although various FPs have been reported,[2] their properties such as protein size and brightness are not completely satisfactory for some biological applications.[1–3] As an alternative to FPs, chemical methods utilizing synthetic fluorescence probes and fusion proteins have recently emerged.[4–7] In this imaging technique, a ligand-binding domain is fused to the protein of interest (POI) as a protein (peptide) tag and is reacted with a fluorophore-conjugated ligand. Thus, the POI is labeled by the fluorophore through the linkage of the tag and the ligand. Representative examples of previously commercialized protein (peptide) tags are the HaloTag,[5] the SNAP tag,[6] and the tetracysteine tag.[7] The key characteristics of these techniques are that POIs are conditionally labeled by the temporal addition of probes, and various fluorophores can easily be incorporated into probes by replacing just the fluorophore moiety. However, since the fluorescence of free probes or probes bound to nontarget biomolecules interfere with the identification of the labeled target protein, thorough washing of cells is necessary to remove free probes. This is a time-consuming process, and incomplete washing causes a decrease in the signal-to-noise ratio. To solve this problem, we have developed protein-labeling probes that do not require any washing procedure for live-cell imaging.

As possible approaches to the problem, we and other groups have reported turn-on fluorescence labeling systems, in which the fluorescence of a probe is quenched in a free state and is recovered in a protein-tag-bound state.[7–11] These fluorogenic probes minimize background fluorescence and overcome the limitation of conventional protein-labeling systems. Although many protein-labeling methods are known, fluorogenic methods that do not require any washing are still restricted to a few protein-tagging systems.[11] Therefore, the further development of novel fluorogenic systems is required. Based on the quenching mechanism of intramolecular association, we have recently created a fluorogenic probe, FCTP, for labeling the photoactive yellow protein (PYP) tag (Scheme 1a).[8] The PYP tag is derived from purple bacteria[12] and binds to the thioester derivatives of 4-hydroxycinnamic acid, a natural cofactor, or 7-hydroxycoumarin through transthioesterification with residue Cys69.[8,13] The small size of the PYP tag (14 kDa; half the size of the green fluorescent protein, GFP) makes this protein particularly interesting, as

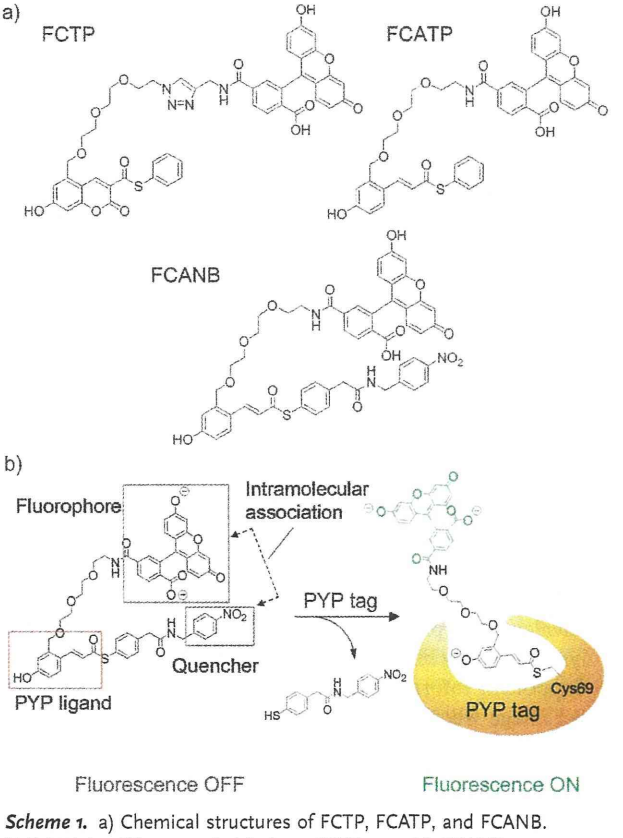


***Scheme 1.*** a) Chemical structures of FCTP, FCATP, and FCANB. b) Principle of fluorogenic labeling of PYP tag with FCANB.

[*] Dr. Y. Hori, K. Nakaki, M. Sato, Dr. S. Mizukami, Prof. K. Kikuchi
Graduate School of Engineering, Osaka University
Osaka 565-0871 (Japan)
E-mail: kkikuchi@mls.eng.osaka-u.ac.jp
Homepage: http://www-molpro.mls.eng.osaka-u.ac.jp/
Dr. S. Mizukami, Prof. K. Kikuchi
Immunology Frontier Research Center, Osaka University
Osaka 565-0871 (Japan)

[**] This work was supported by MEXT of Japan (Grants 20675004, 22108519 to K.K. and 22685016, 23114710 to Y.H.), by the Funding Program for World-Leading Innovative R&D on Science and Technology from JSPS, by the Grant-in-Aid from the Ministry of Health, Labour and Welfare (MHLW) of Japan, by CREST from JST, and by Asahi Glass Foundation.

Supporting information (including experimental details) for this article is available on the WWW under http://dx.doi.org/10.1002/anie.201200867.

well as promising for protein-tagging technology. Other than the tetracysteine tag, the PYP tag is the smallest protein tag covalently labeled by a fluorogenic substrate. The fluorogenic probe FCTP is nonfluorescent because of the intramolecular association between the fluorescein and coumarin moieties, but the fluorescence is restored by the reversal of this association upon protein labeling. The probe FCTP, however, requires more than 24 h to complete this labeling reaction. For this reason, a washing step is essential for expeditious live-cell imaging with a high signal-to-noise ratio. Hence, fluorogenic probes with much more rapid kinetics are required for no-wash imaging.

To achieve this, we have employed a design strategy based on a new probe scaffold consisting of cinnamic acid thioester as a PYP-tag ligand and nitrobenzene as a fluorescence quencher (Scheme 1). By introducing fluorescein as a fluorophore into this scaffold, we have designed and synthesized a fluorogenic probe, FCANB. Cinnamic acid thioester was chosen in place of the coumarin ligand, which had been utilized in FCTP, to reduce the intramolecular stacking interaction between the ligand and fluorophore moieties. This interaction is undesirable, because it could cause steric hindrance around the ligand toward the PYP tag, and this hindrance was observed for FCTP in our previous study.[8] Nitrobenzene has desirable properties as a fluorogenic switch. The first is a synthetic advantage, in that it is easily incorporated into fluorescence probes owing to its simple structure. A more important feature is that nitrobenzene associates with fluorophores, including fluorescein, and thereby quenches the fluorescence.[9,14] Furthermore, this quenching mechanism can be utilized as a general strategy for the design of turn-on fluorescence probes. It is envisioned that the fluorescein of the probe loses its fluorescence by the association with nitrobenzene, and this association inhibits the unwanted interaction between the ligand and fluorophore moieties, thereby leading to rapid protein labeling (Scheme 1b). Moreover, the probe will become fluorescent if the thiophenyl leaving group that is connected to nitrobenzene is dissociated from the probe upon protein labeling. To confirm the effects of nitrobenzene, we have also synthesized a probe, FCATP, which does not contain nitrobenzene (Scheme 1a).

First, the binding characteristics of the probes with the PYP tag were investigated. Purified PYP tag was incubated with the probes FCATP or FCANB and analyzed by SDS-PAGE after heating at 95 °C. In both cases, a fluorescent band appeared in the gel and the molecular weight was in accordance with that of the PYP tag, thus indicating that the probes bind to PYP tag (Figure 1a, Figure S1 in the Supporting Information). Since the samples were denatured by SDS and heat, the binding mode is considered to be covalent. The probes were also reacted with PYP tag in cell lysate to verify binding specificity (Figure 1b, Figure S1 in the Supporting Information). No fluorescence was detected in the gel image when the probes were added to cell lysate in the absence of PYP tag. In contrast, in the case of PYP-tag-containing cell lysate, a single fluorescent band appeared in the gel at the band position of the PYP tag. These results confirm that the probes specifically bind to the PYP tag.

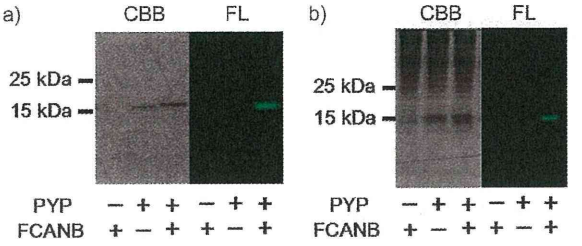


***Figure 1.*** SDS-PAGE experiments of labeling reactions of PYP tag with the probe FCANB. Images of Coomassie Brilliant Blue (CBB)-stained and fluorescence gel are displayed on the left and right, respectively. PYP tag (a: 10 μM, b: 5 μM) was reacted with FCANB (a: 16 μM, b: 8 μM). Images (a) and (b) represent the reactions in the absence and presence of cell lysate, respectively.

Next, fluorescence spectra were measured to examine whether the fluorescence intensity of the probes increased upon binding to the PYP tag (Figure 2a, Table 1). Unexpectedly, FCATP exhibited only a slight fluorescence in the absence of PYP tag (fluorescence quantum yield $\Phi_f = 0.05$), even though no quenching group was introduced into this molecule. The binding of FCATP to the PYP tag led to a 9.3-fold enhancement of the fluorescence. Similarly, the fluores-

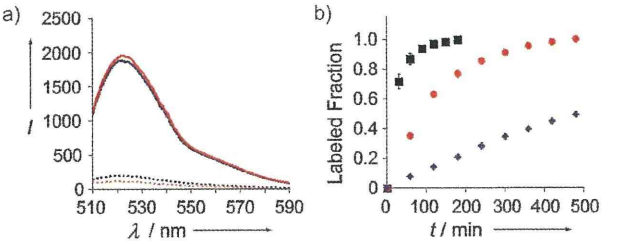


***Figure 2.*** Fluorescence spectroscopy analyses of labeling reactions. a) Fluorescence emission spectra of FCATP (blue lines) and FCANB (red lines) in the absence (dotted lines) or presence (solid lines) of PYP tag. b) Time course of labeling reactions of FCTP (blue diamonds), FCATP (red circles), and FCANB (black squares) with PYP tag. All measurements were conducted using samples in tris(hydroxymethyl)aminomethane hydrochloride (Tris) buffer (20 mM Tris·HCl, 150 mM NaCl (pH 7.4)) at 37 °C. The probe and protein concentrations were 8 μM.

***Table 1:*** Spectral and kinetic properties of PYP-tag probes.

| Probe | $\lambda_{abs}$ [nm] | $\lambda_{em}$ [nm] | $\varepsilon$ [$M^{-1}cm^{-1}$] | $\Phi_f$ | $k_2$[a] [$M^{-1}s^{-1}$] |
|---|---|---|---|---|---|
| FCTP | 505 | 522 | 37300 | 0.02 | 1.11 |
| FCATP | 501 | 522 | 51100 | 0.05 | 11.1 |
| FCANB | 501 | 521 | 44400 | 0.04 | 125 |
| Probe–PYP tag[b] | 498 | 521 | 57300 | 0.47 | – |

[a] All measurements were made in triplicate. $k_2$ = second-order rate constant. [b] Spectroscopic data of PYP-tag-bound probe were obtained after the labeling reaction of PYP tag with FCANB was completed.

cence intensity of FCANB was weak ($\Phi_f = 0.04$) and was augmented by the binding of FCANB to the PYP tag ($\Phi_f = 0.47$); its fluorescence change was 15-fold and thus larger than that of FCATP. Neither of the probes displayed a time-dependent alteration of the fluorescence intensity in the absence of PYP tag (Figure S2 in the Supporting Information). These results demonstrate that both FCATP and FCANB are fluorogenic probes for labeling PYP tag. Moreover, they show that the nitrobenzene moiety in FCANB contributes to the quenching efficiency by lowering the fluorescence quantum yield and extinction coefficient of the fluorophore under these experimental conditions (Table 1). The absorption spectra of free FCATP and FCANB show that the maximum wavelength was shifted by 7 nm in comparison to that of the fluorescein derivative without a ligand or nitrobenzene moiety (Figure S3 in the Supporting Information). This spectral change strongly suggests that intramolecular association occurs between the fluorophore and the ligand or nitrobenzene, and this association could cause fluorescence quenching for both probes. This type of quenching mechanism has also been reported, and it has been shown that fluorescence quenching is triggered by the close contact of intramolecular fluorophores.[8,15]

The kinetic analyses of protein labeling were carried out by monitoring the increase in the fluorescence intensity of the probes. The time required for 50% labeling, $t_{1/2}$, was estimated using the labeling reactions, in which the concentrations of the probes and proteins were 8 μM (Figure 2b, Figure S2 in the Supporting Information). FCANB has the shortest $t_{1/2}$ value (ca. 15 min), followed by FCATP ($t_{1/2}$ ca. 78 min) and FCTP ($t_{1/2} > 470$ min), thus demonstrating that FCANB binds to the PYP tag most rapidly. In further kinetic analyses, second-order rate constants were also calculated (Table 1, Figure S4 in the Supporting Information). Consistent with the $t_{1/2}$ values, the $k_2$ values of FCATP and FCANB are 10-fold and 110-fold higher than that of FCTP, respectively. These kinetic data suggest that the introduction of the 4-hydroxycinnamic acid ligand in probes FCATP and FCANB leads to the fast protein labeling. There is a possibility that the PYP tag could intrinsically bind to the 4-hydroxycinnamic acid ligand more rapidly than to the coumarin ligand. However, this possibility was excluded, because it was found that the PYP tag binds to both ligands, neither of which contains the fluorophore, with almost the same kinetics (Figure S5 in the Supporting Information). Therefore, it is more likely that the strength of intramolecular interaction or the structure of the intramolecular complex between the fluorophore and ligand moieties affects the protein-labeling kinetics of both probes FCANB and FCATP. As well as the 4-hydroxycinnamic acid ligand, nitrobenzene also gave a promotional effect on the protein labeling kinetics of FCANB, as expected. This result suggests that the fluorophore interacts more favorably with the nitrobenzene rather than with the ligand moiety, and thereby the steric hindrance around the ligand is diminished.

Finally, live-cell imaging was conducted using the probes. Epidermal growth factor receptor (EGFR) fused with the PYP tag at the N-terminal extracellular domain (PYP–EGFR) was expressed on the surface of human embryonic kidney (HEK293T) cells (Figure S6 in the Supporting Information), and each of the probes was incubated with the cells for 30 min. After washing the cells to remove free probes, fluorescence images were taken using confocal laser-scanning microscopy (Figure 3a, Figure S7a in the Supporting Information). Clear fluorescence was observed along the plasma membrane in the cells treated with either FCATP or FCANB. No fluorescence was detected in cells expressing EGFR without PYP tag. These results indicate that both probes specifically label the PYP–EGFR fusion protein on the cell surface. We also tried to label PYP-tagged proteins inside cells with the probes. This attempt, however, failed, because the probes were not cell-permeable. Taking advantage of the fluorogenic properties of the probes, direct imaging of cell-surface proteins without washing was performed immediately after the labeling reaction (Figure 3b, Figure S7b). As in images obtained when the washing procedure was used, distinct fluorescence was detected only on the surface of the cells expressing the PYP–EGFR fusion protein, while the fluorescence of the free probe was not seen in the media or in other parts of cells. Nonspecific labeling was also confirmed to be absent in cells that do not express the PYP–EGFR fusion protein. Importantly, specific imaging of proteins was accomplished by utilizing these fluorogenic probes without washing.

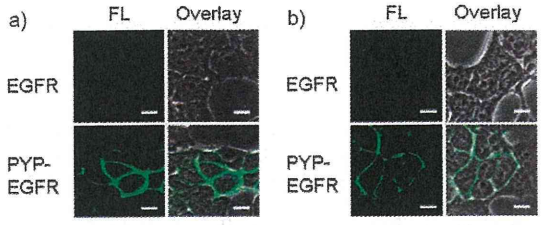


***Figure 3.*** Live-cell imaging of PYP-tagged EGFR on cell surfaces with the probe FCANB (5 μM) a) with or b) without washing procedures. Fluorescence images and their overlays with phase contrast images are shown in the left and right of each panel, respectively. Scale bars: 10 μm.

In summary, we have developed fluorogenic probes, FCATP and FCANB, for labeling PYP tag. Kinetic properties of the probes were significantly improved compared to the previous probe, FCTP. In particular, FCANB binds to the PYP tag 110 times more rapidly than FCTP. This acceleration effect is induced by the introduction of both the cinnamic acid ligand and the nitrobenzene quencher into the probe structure. A possible reason for this effect is that the fluorophore preferably interacts with the nitrobenzene instead of the ligand and that thereby the steric hindrance around the ligand is reduced. The kinetic enhancement and fluorogenicity of the probes enabled the specific labeling of PYP-tagged proteins on the cell surface with a procedure that does not require washing steps. The most notable point is that the PYP tag is the smallest protein among existing protein tags that can be covalently labeled by small fluorogenic compounds without the requirement of washing cells. This no-wash labeling system combined with the small PYP tag offers an attractive tool for the imaging of rapid movement and

trafficking of cell-membrane proteins with a high signal-to-noise ratio.

Received: February 1, 2012
Revised: March 19, 2012
Published online: ■■ ■■, ■■■■

**Keywords:** fluorescence imaging · fluorescent probes · intramolecular association · protein modifications · protein tags

[1] A. Miyawaki, *Nat. Rev. Mol. Cell Biol.* **2011**, *12*, 656–668.
[2] a) J. Wiedenmann, F. Oswald, G. U. Nienhaus, *IUBMB Life* **2009**, *61*, 1029–1042; b) D. M. Chudakov, M. V. Matz, S. Lukyanov, K. A. Lukyanov, *Physiol. Rev.* **2010**, *90*, 1103–1163.
[3] a) C. L. Thomas, A. J. Maule, *J. Gen. Virol.* **2000**, *81*, 1851–1855; b) C. S. Lisenbee, S. K. Karnik, R. N. Trelease, *Traffic* **2003**, *4*, 491–501; c) P. R. Dahlgren, M. A. Karymov, J. Bankston, T. Holden, P. Thumfort, V. M. Ingram, Y. L. Lyubchenko, *Nanomedicine* **2005**, *1*, 52–57; d) A. Raney, A. Y. Shaw, J. L. Foster, J. V. Garcia, *Virology* **2007**, *368*, 7–16.
[4] a) Y. Yano, K. Matsuzaki, *Biochim. Biophys. Acta Biomembr.* **2009**, *1788*, 2124–2131; b) C. Jing, V. W. Cornish, *Acc. Chem. Res.* **2011**, *44*, 784–792; c) M. W. Popp, J. M. Antos, G. M. Grotenbreg, E. Spooner, H. L. Ploegh, *Nat. Chem. Biol.* **2007**, *3*, 707–708; d) H. Nonaka, S. Tsukiji, A. Ojida, I. Hamachi, *J. Am. Chem. Soc.* **2007**, *129*, 15777–15779; e) S. S. Gallagher, J. E. Sable, M. P. Sheetz, V. W. Cornish, *ACS Chem. Biol.* **2009**, *4*, 547–556; f) Y. Hori, Y. Egashira, R. Kamiura, K. Kikuchi, *ChemBioChem* **2010**, *11*, 646–648.
[5] a) G. V. Los, K. Wood, *Methods Mol. Biol.* **2007**, *356*, 195–208; b) H. L. Lee, S. J. Lord, S. Iwanaga, K. Zhan, H. Xie, J. C. Williams, H. Wang, G. R. Bowman, E. D. Goley, L. Shapiro, R. J. Twieg, J. Rao, W. E. Moerner, *J. Am. Chem. Soc.* **2010**, *132*, 15099–15101.
[6] a) A. Keppler, S. Gendreizig, T. Gronemeyer, H. Pick, H. Vogel, K. Johnsson, *Nat. Biotechnol.* **2003**, *21*, 86–89; b) A. Gautier, A. Juillerat, C. Heinis, I. R. Correa, Jr., M. Kindermann, F. Beaufils, K. Johnsson, *Chem. Biol.* **2008**, *15*, 128–136.
[7] a) B. A. Griffin, S. R. Adams, R. Y. Tsien, *Science* **1998**, *281*, 269–272; b) S. R. Adams, R. E. Campbell, L. A. Gross, B. R. Martin, G. K. Walkup, Y. Yao, J. Llopis, R. Y. Tsien, *J. Am. Chem. Soc.* **2002**, *124*, 6063–6076; c) M. J. Roberti, C. W. Bertoncini, R. Klement, E. A. Jares-Erijman, T. M. Jovin, *Nat. Methods* **2007**, *4*, 345–351.
[8] Y. Hori, H. Ueno, S. Mizukami, K. Kikuchi, *J. Am. Chem. Soc.* **2009**, *131*, 16610–16611.
[9] K. K. Sadhu, S. Mizukami, S. Watanabe, K. Kikuchi, *Chem. Commun.* **2010**, *46*, 7403–7405.
[10] S. Mizukami, S. Watanabe, Y. Hori, K. Kikuchi, *J. Am. Chem. Soc.* **2009**, *131*, 5016–5017.
[11] a) T. Komatsu, K. Johnsson, H. Okuno, H. Bito, T. Inoue, T. Nagano, Y. Urano, *J. Am. Chem. Soc.* **2011**, *133*, 6745–6751; b) X. Sun, A. Zhang, B. Baker, L. Sun, A. Howard, J. Buswell, D. Maurel, A. Masharina, K. Johnsson, C. J. Noren, M. Q. Xu, I. R. Corrêa, Jr., *ChemBioChem* **2011**, *12*, 2217–2226; c) C. J. Zhang, L. Li, G. Y. Chen, Q. H. Xu, S. Q. Yao, *Org. Lett.* **2011**, *13*, 4160–4163.
[12] a) T. E. Meyer, *Biopchim. Biophys. Acta* **1985**, *806*, 175–183; b) M. Kumauchi, M. T. Hara, P. Stalcup, A. Xie, W. D. Hoff, *Photochem. Photobiol.* **2008**, *84*, 956–969.
[13] a) Y. Imamoto, T. Ito, M. Kataoka, F. Tokunaga, *FEBS Lett.* **1995**, *374*, 157–160; b) W. D. Hoff, B. Devreese, R. Fokkens, I. M. Nugteren-Roodzant, J. Van Beeumen, N. Nibbering, K. J. Hellingwerf, *Biochemistry* **1996**, *35*, 1274–1281; c) R. Cordfunke, R. Kort, A. Pierik, B. Gobets, G.-J. Koomen, J. W. Verhoeven, K. J. Hellingwerf, *Proc. Natl. Acad. Sci. USA* **1998**, *95*, 7396–7401.
[14] G. S. Beddard, S. Carlin, L. Harris, G. Porter, C. J. Tredwell, *Photochem. Photobiol.* **1978**, *27*, 433–438.
[15] a) A. P. Wei, D. K. Blumenthal, J. N. Herron, *Anal. Chem.* **1994**, *66*, 1500–1506; b) B. Z. Packard, D. D. Toptygin, A. Komoriya, L. Brand, *Proc. Natl. Acad. Sci. USA* **1996**, *93*, 11640–11645; c) H. Takakusa, K. Kikuchi, Y. Urano, T. Higuchi, T. Nagano, *Anal. Chem.* **2001**, *73*, 939–942.

  